A novel somatic *FGFR3* mutation in primary lung cancer

KAZUYA SHINMURA[1], HISAMI KATO[1], SHUN MATSUURA[1,2], YUSUKE INOUE[1,2], HISAKI IGARASHI[1], KIYOKO NAGURA[1], SATOKI NAKAMURA[1], KYOKO MARUYAMA[1], MARI TAJIMA[1], KAZUHITO FUNAI[3], HIROSHI OGAWA[4], MASAYUKI TANAHASHI[5], HIROSHI NIWA[5] and HARUHIKO SUGIMURA[1]

Departments of [1]Tumor Pathology, [2]Internal Medicine 2 and [3]Surgery 1, Hamamatsu University School of Medicine, Hamamatsu, Shizuoka 431-3192; Divisions of [4]Pathology and [5]Thoracic Surgery, Respiratory Disease Center, Seirei Mikatahara General Hospital, Hamamatsu, Shizuoka 433-8558, Japan

Received October 9, 2013; Accepted November 25, 2013

DOI: 10.3892/or.2014.2984

Abstract. The recent discovery of mutations and fusions of oncokinase genes in a subset of lung cancers (LCs) is of considerable clinical interest, since LCs containing such mutations or fusion transcripts are reportedly sensitive to kinase inhibitors. To better understand the role of the recently identified fibroblast growth factor receptor 3 (*FGFR3*) mutations and fusions in pulmonary carcinogenesis, we examined 214 LCs for mutations in the mutation cluster region of the *FGFR3* gene using sequencing analysis. We also examined 190 LCs for the FGFR3-TACC3 and FGFR3-BAIAP2L1 fusion transcripts using reverse transcription-polymerase chain reaction (RT-PCR) analysis. Although the expression of FGFR3-TACC3 and FGFR3-BAIAP2L1 fusion transcripts was not detected in any of the carcinomas, somatic *FGFR3* mutations were detected in two (0.9%) LCs. The two mutations were the same, i.e., p.R248H. That was a novel mutation occurring in the same codon as p.R248C, for which an oncogenic potential has previously been shown. Increased FGFR3 expression was shown in the two LCs containing the *FGFR3* p.R248H mutation using qPCR. Histologically, both carcinomas were squamous cell carcinomas, therefore the incidence of the *FGFR3* mutation among the squamous cell carcinoma cases was calculated as 3.2% (2/63). When we examined other co-occurring genetic abnormalities, one case exhibited a *p53* p.R273C mutation, while the other case exhibited *PIK3CA* and *SOX2* amplifications. The above results suggest that an *FGFR3* p.R248H mutation is involved in the carcinogenesis of a subset of LCs and may contribute to the elucidation of the characteristics of *FGFR3* mutation-positive LCs in the future.

Correspondence to: Dr Kazuya Shinmura, Department of Tumor Pathology, Hamamatsu University School of Medicine, 1-20-1 Handayama, Higashi Ward, Hamamatsu, Shizuoka 431-3192, Japan
E-mail: kzshinmu@hama-med.ac.jp

Key words: fibroblast growth factor receptor 3, somatic mutation, fusion gene, lung cancer, squamous cell carcinoma

Introduction

Mutations of *EGFR*, *KRAS*, *PIK3CA*, and others, and fusion transcripts of ALK, ROS1 and RET are oncogenic alterations in lung cancers (LCs) and some of them are therapeutic targets (1-8). For example, crizotinib, a small molecule inhibitor of ALK, has been shown to selectively inhibit the growth of ALK-positive LC (9), meaning that a subclass of LC patients are likely to benefit clinically from an ALK inhibitor. Therefore, targetable oncogenic alterations in LCs may have a significant clinical impact.

Fibroblast growth factor receptor 3 (FGFR3) has been revealed to be activated by the mutation or fusion of its own gene in several types of cancer, such as urinary bladder cancer, glioblastoma, rhabdomyosarcoma and LC (10-17). Some tumor-specific *FGFR3* mutations, including p.R248C and p.S249C, drive the anchorage-independent growth of NIH3T3 cells and tumor formation in xenograft models, and cells harboring such *FGFR3* mutations showed an enhanced sensitivity to BGJ398, a selective FGFR kinase inhibitor (17). Regarding fusions, FGFR3-TACC3 and FGFR3-BAIAP2L1 oncogenic fusions have thus far been identified (13-15), and cells harboring the FGFR3-TACC3 fusion showed enhanced sensitivity to three FGFR kinase inhibitors, including BGJ398 (13). Thus, oncogenic *FGFR3* mutations and fusions in tumors can be therapeutic targets. To determine which patients can benefit from FGFR inhibitors in the future, the incidence of *FGFR3* mutations or fusions in various tumors derived from patients from various demographic areas must be determined. However, to date, only a few studies have been published regarding *FGFR3* mutations and fusions in LC and Asian patients with LC have not yet been analyzed (12,16,17). Notably, according to previous reports (12,16,17), the only experimentally proven oncogenic *FGFR3* mutations in LCs are p.R248C and p.S249C, which are located within the first ten bases of exon 7. Therefore, we considered this region to be a mutation cluster region in LCs. In the present study, to determine the status of *FGFR3* mutation and fusion in LCs derived from Japanese patients, we examined LCs from Japanese patients for the mutations in the mutation cluster region of *FGFR3* and the expression of FGFR3-TACC3 and FGFR3-BAIAP2L1 fusion transcripts and pathologically and molecularly characterized LCs containing such an alteration.

This is the first published study to describe *FGFR3* mutations in LCs derived from Japanese patients.

Materials and methods

Primary LC. Samples of surgical specimens were obtained from 362 Japanese LC patients who underwent surgery for cancer at Hamamatsu University Hospital and Mikatahara Seirei General Hospital. Informed consent was obtained from all the patients, and the study was approved by the Institutional Review Boards (IRBs) of Hamamatsu University School of Medicine and Mikatahara Seirei General Hospital. The clinicopathological profiles of the cases are shown in Table I. The histological classification was based on the World Health Organization system. Among the 362 cases, 214 cases were used in the mutational analysis, whereas 190 cases were used in the reverse transcription-polymerase chain reaction (RT-PCR) analysis; 42 cases were used in both analyses.

Search for FGFR3 mutations using PCR-sequencing. Genomic DNAs were extracted from the lung tissue samples using a DNeasy kit (Qiagen, Valencia, CA, USA) and were examined for somatic mutations in the DNA sequences (the first half of exon 7) covering the mutation cluster region in the *FGFR3* gene. PCR was performed in 20-μl reaction mixtures containing HotStarTaq DNA polymerase (Qiagen) under the following conditions: 30 sec at 94°C, 30 sec at 65°C and 60 sec at 72°C for 45 cycles. The following set of primers was used: 5'-CTG AGC GTC ATC TGC CCC C-3' and 5'-TGG GGC TGT GCG TCA CTG TAC-3'. PCR-amplified products were purified with ExoSAP-IT (GE Healthcare Bio-Sciences, Piscataway, NJ, USA) and were sequenced directly using a BigDye Terminator Cycle Sequencing Reaction kit (Applied Biosystems, Tokyo, Japan) and the ABI 3130 Genetic Analyzer (Applied Biosystems).

Search for FGFR3 fusion transcripts using RT-PCR. Total RNA was extracted from the lung tissue samples using an RNeasy kit (Qiagen) and was converted to first-strand cDNA using a SuperScript First-Strand Synthesis System for RT-PCR (Invitrogen, Carlsbad, CA, USA) according to the supplier's protocol. PCR was performed in 20-μl reaction mixtures containing HotStarTaq DNA polymerase under the following conditions: 30 sec at 94°C, 30 sec at 59°C and 60 sec at 72°C for 45 cycles. The following reverse PCR primers were used: 5'-CAG CCT CCA CTG GTT TCT GTA G-3' for the sequence at exon 4 of TACC3, 5'-TGG TAC ACA ACC TCT TCG AAC C-3' for the sequence at exon 12 of TACC3, and 5'-GGA CAT GTC CCA GTT CAG TTG-3' for the sequence at exons 3 and 4 of BAIAP2L1. The forward PCR primer used was the same, i.e., 5'-GAC CGT GTC CTT ACC GTG AC-3' for the sequence at exon 18 of FGFR3. The PCR products were fractionated using electrophoresis on an agarose gel and were stained with ethidium bromide.

Quantitative RT (qRT)-PCR. The expressions of the FGFR3 mRNA transcripts were measured using real-time qRT-PCR with a LightCycler instrument (Roche, Palo Alto, CA, USA). PCR amplification of the FGFR3 transcript and the transcript of the control housekeeping gene *GAPDH* was performed with the cDNA and a QuantiTect SYBR Green PCR kit (Qiagen). The following PCR primers were used: 5'-GCA CAC ACG ACC TGT ACA TGA TC-3' and 5'-CCA GGT ACT CGT CGG TGG AC-3' for the FGFR3 transcript, and 5'-GCT CAG ACA CCA TGG GGA AG-3' and 5'-TGT AGT TGA GGT CAA TGA AGG GG-3' for the GAPDH transcript. The T/N ratios were calculated by dividing the normalized transcript amounts in the cancerous tissue by the amounts in the non-cancerous tissue.

Table I. Summary of the clinicopathological profiles of the patients.

Characteristics	Number[a]		
	Total	Mutational analysis	RT-PCR analysis
No. of patients	362	214	190
Age, years (mean ± SD)	66.5±9.6	66.4±9.7	66.9±9.9
Gender, n (%)			
Male	259 (71.5)	157 (73.4)	134 (70.5)
Female	103 (28.5)	57 (26.6)	56 (29.5)
Histology, n (%)			
Adenocarcinoma	210 (58.0)	125 (58.4)	109 (57.4)
Squamous cell carcinoma	110 (30.4)	63 (29.4)	60 (31.6)
Large cell carcinoma	13 (3.6)	9 (4.2)	5 (2.6)
Small cell carcinoma	12 (3.3)	11 (5.1)	3 (1.6)
Adenosquamous carcinoma	11 (3.0)	4 (1.9)	9 (4.7)
Pleomorphic carcinoma	6 (1.7)	2 (0.9)	4 (2.1)

[a]Forty-two cases were used in both the mutational analysis and the RT-PCR analysis. SD, standard deviation. RT-PCR, reverse transcription-polymerase chain reaction.

Immunohistochemical staining. Sections of formalin-fixed, paraffin-embedded tissue samples were used for immunohistochemical staining using a Histofine Simple Stain MAX PO kit (Nichirei, Tokyo, Japan), as previously described (18). The primary antibodies were: anti-CK14, anti-thyroid transcription factor-1 (TTF-1) (both from Novocastra Laboratories, Newcastle, UK) and anti-p53 (clone DO7; Dako, Tokyo, Japan). Hematoxylin and eosin (H&E) staining was also performed.

Search for EGFR, KRAS, PIK3CA and p53 mutations using PCR-sequencing. Genomic DNA derived from the lung tissue samples containing an *FGFR3* mutation was examined for somatic mutations in the DNA sequences of mutation cluster regions in the *EGFR*, *KRAS*, *PIK3CA* and *p53* genes. PCR amplification was performed as previously described (7). Sequencing was performed as described in the 'Search for *FGFR3* mutations using PCR-sequencing' section.

Fluorescence in situ hybridization (FISH) analysis. Paraffin-embedded tissue sections were de-waxed and re-hydrated, then

boiled in 0.01 M citrate buffer (pH 6.0) to release the closed chromosomal structures. A combination of Cy3-labeled bacterial artificial chromosome (BAC) clone (RP11-100B16) for the *FGFR1* locus, BAC clone (RP11-245C23 and RP11-355N16) for the *PIK3CA* locus, or BAC clone (RP11-275H4) for the *SOX2* locus and a SpectrumGreen-labeled control BAC probe for the near centromere locus on chromosome 3 or 8 were placed on a slide and covered with a coverslip. All the BAC probes were obtained from Advanced GenoTechs Co. (Tsukuba, Japan). The slides with the hybridization mixture were denatured on a digital hot plate (HP-15; As One Corporation, Osaka, Japan) and then incubated overnight at 42˚C. After washing the slide in 50% formamide/2X SSC, mounting medium containing DAPI (Vector Laboratories, Burlingame, CA, USA) was used for nuclear counterstaining. The slides were promptly examined under a fluorescence microscope (Olympus BX51-FL; Olympus, Tokyo, Japan) equipped with epifluorescence filters and a photometric CCD camera (Sensicam; PCO Company, Kelheim, Germany). The images captured were digitized and stored in the image analysis program (MetaMorph; Molecular Devices, Palo Alto, CA, USA). The average ratio of the *FGFR1*, *PIK3CA*, or *SOX2* signal number to the control probe signal number was calculated for each cancer. If the ratio of a cancer was >2.5, the cancer was defined as amplification-positive.

Results

In the present study, we examined 214 LCs for mutations in the mutation cluster region of the *FGFR3* gene using a sequencing analysis; we also examined 190 LCs for FGFR3-TACC3 and FGFR3-BAIAP2L1 fusion transcripts using an RT-PCR analysis. Although the expression of FGFR3-TACC3 and FGFR3-BAIAP2L1 fusion transcripts was not detected in any of the carcinomas, *FGFR3* mutations were detected in two (0.9%) LCs (Fig. 1A). The mutations that occurred in the LCs derived from cases no. 57 and no. 183 were the same, i.e., a somatic c.743G>A mutation associated with an amino acid exchange from Arg to His at codon 248. The p.R248H mutation in the *FGFR3* gene has not been previously reported, suggesting it is a novel mutation. Of note, with regards to codon 248, it was previously reported that the p.R248C mutation drives cellular transformation (17), indicating that the p.R248H mutation may have an oncogenic potential similar to that of the p.R248C mutation. When we next examined the expression levels of FGFR3 mRNA transcripts in the two LCs containing an *FGFR3* p.R248H mutation using a qRT-PCR analysis, the ratio of the level of FGFR3 mRNA expression in the cancerous tissue to the level in the corresponding non-cancerous tissue (T/N ratio) was increased in both cases (Fig. 1B), suggesting the involvement of mutated FGFR3 in LC. Case no. 57 was a 62-year-old man who was a smoker [Brinkman index (BI)=1,800] and case no. 183 was a 66-year-old man who was also a smoker (BI=1,000). The histological classification of both LCs was squamous cell carcinoma (Fig. 2A and B). An immunohistochemical study revealed that the carcinomas were positive for CK14 but negative for TTF-1 (Fig. 2C and D, Table II), indicating that the immunophenotype of the carcinoma was compatible with that of squamous cell carcinoma. Among the 214 cases used for the mutational analysis, 63 cases were histologically classified as

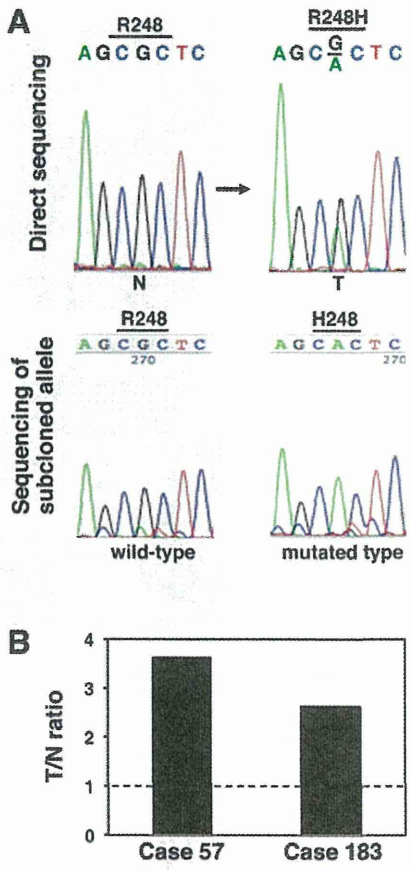

Figure 1. Detection of *FGFR3* mutations in primary lung cancer (LC). (A) Results of direct sequencing analysis of the *FGFR3* gene in LC DNA derived from case no. 183 (upper panels) and results of sequencing analysis of the subcloned PCR product covering the mutation in the case (lower panels). A somatic CGC to CAC mutation associated with the conversion from Arg to His at codon 248 was detected in the LC. N, non-cancerous lung tissue DNA; T, cancerous lung tissue DNA. In the analysis of subcloned products, both wild-type and mutated-type alleles were detected. (B) Comparison between FGFR3 mRNA expression in cancerous tissues from two LCs containing an *FGFR3* mutation and corresponding non-cancerous lung tissues, as determined using a qRT-PCR analysis. After normalizing the amounts of FGFR3 transcripts to those of the GAPDH transcripts, the T/N values were calculated by dividing the amount of normalized transcripts in the cancerous tissue by the amount in the corresponding non-cancerous tissue. FGFR3, fibroblast growth factor receptor 3.

squamous cell carcinoma; thus, the incidence of the *FGFR3* mutation among the squamous cell carcinoma cases was 3.2% (2/63). These findings suggest that a subset of LC may carry an *FGFR3* mutation.

We next examined whether the LC cases containing the *FGFR3* p.R248H mutation also contained mutations in other genes that are often mutated in LC (3,8,12,19,20). Mutation cluster regions for *EGFR*, *KRAS*, *PIK3CA* and *p53* (3,8,12,19,20) were searched for somatic mutations. No somatic mutations in exon 2 of *KRAS*, exons 19 and 21 of *EGFR*, or exons 9 and 20 of *PIK3CA* were detected; however, a somatic c.817C>T mutation associated with an amino acid exchange from Arg to Cys at codon 273 (p.R273C) was detected in the *p53* gene in case no. 183 (Fig. 2E, Table II). The fact that the missense mutation was detected in the DNA binding region of the p53 protein suggested that the mutant p53 protein was stable in the cancer

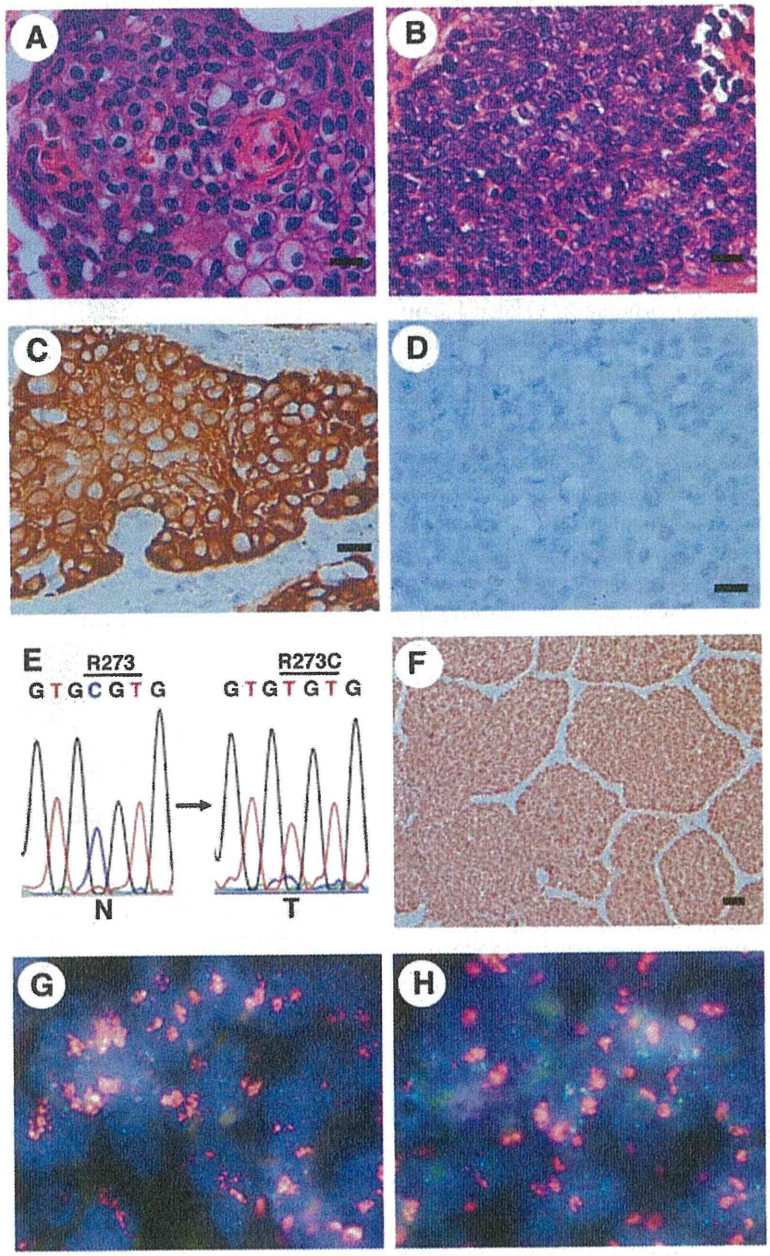

Figure 2. Pathological, immunohistochemical, mutational and FISH analyses for lung cancers (LCs) containing an *FGFR3* mutation. (A and B) Microscopic image (H&E) of the squamous cell carcinoma in case no. 57 (A) and case no. 183 (B). Scale bar, 20 μm. (C and D) The squamous cell carcinoma of case no. 57 was immunohistochemically positive for CK14 (C) and negative for TTF-1 (D). Scale bar, 20 μm. (E) Detection of a somatic *p53* missense mutation in LC from case no. 183. A CGT to TGT mutation associated with the conversion from Arg to Cys at codon 273 was detected in the LC. N, non-cancerous lung tissue DNA; T, cancerous lung tissue DNA. (F) Immunohistochemical detection of p53 accumulation in the LC from case no. 183. Scale bar, 50 μm. (G and H) *PIK3CA* (G) and *SOX2* (H) amplifications in LC from case no. 57, as shown using a FISH analysis. Red signals, BAC probe for the *PIK3CA* (G) and *SOX2* (H) locus; green signals, control probe for the near centromere locus on chromosome 3. FGFR3, fibroblast growth factor receptor 3; H&E, hematoxylin and eosin; TTF-1, thyroid transcription factor-1.

cells. We therefore performed immunohistochemical staining for p53 in case no. 183 and the results showed the nuclear accumulation of p53 exclusively in the cancer cells (Fig. 2F). These results suggested that a somatic *p53* mutation, but not *EGFR*, *KRAS* or *PIK3CA* mutations, may occur in a subset of LCs containing an *FGFR3* mutation.

We also examined whether the LC cases containing the *FGFR3* p.R248H mutation also contained gene amplifications, which are frequently observed in LC (12,21,22). The amplification status of the *FGFR1*, *PIK3CA* and *SOX2* genes was examined using a FISH analysis. Although *FGFR1* amplification was not detected in either case, the amplification of the *PIK3CA* and *SOX2* genes was detected in case no. 57 (Fig. 2G and H, Table II). These results suggested that *PIK3CA* and *SOX2* gene amplification, but not *FGFR1*, may occur in a subset of LCs containing an *FGFR3* mutation.

Table II. Clinical profiles of the cases with LC containing an *FGFR3* mutation and the pathological, immunohistochemical, mutational and amplification status of the LCs.

Characteristics	Case No. 57	Case No. 183
FGFR3 mutation	p.R248H	p.R248H
Age (years)	62	66
Gender	Male	Male
Smoking habit	Smoker (BI=1,800)	Smoker (BI=1,000)
Histology	Squamous cell carcinoma	Squamous cell carcinoma
Stage	III	II
Lymph node metastasis	Positive	Positive
CK14 expression	Positive	Positive
TTF-1 expression	Negative	Negative
EGFR mutation (exons 19 and 21)	Wild-type	Wild-type
KRAS mutation (exon 2)	Wild-type	Wild-type
PIK3CA mutation (exons 9 and 20)	Wild-type	Wild-type
p53 mutation (exons 4-9)	Wild-type	p.R273C mutation
FGFR1 amplification	Amplification (-)	Amplification (-)
PIK3CA amplification	Amplification (+)	Amplification (-)
SOX2 amplification	Amplification (+)	Amplification (-)

BI, Brinkman index; LC, lung cancer; FGFR3, fibroblast growth factor receptor 3;TTF-1, thyroid transcription factor-1.

Discussion

In the present study, *FGFR3* mutations were found in two (0.9%) of the 214 LCs that were examined, but the expression of FGFR3-TACC3 and FGFR3-BAIAP2L1 fusion transcripts was not detected in any of the 190 LCs that were examined. Both LCs containing an *FGFR3* mutation were histologically diagnosed as squamous cell carcinoma, and squamous cell carcinoma accounted for 63 out of the 214 LCs examined in the mutational analysis, resulting in an incidence of *FGFR3* mutation among squamous cell carcinoma cases of 3.2% (2/63). Both of the mutations were p.R248H, which was a novel mutation located in the same codon as the oncogenic p.R248C mutation. Both LCs exhibited an increased FGFR3 expression, suggesting the involvement of mutated FGFR3 in LC. Regarding the co-occurring genetic abnormalities, one case exhibited a *p53* p.R273C mutation, while the other case exhibited *PIK3CA* and *SOX2* amplifications. No somatic mutations were detected in the mutation cluster regions of the *EGFR*, *KRAS* and *PIK3CA* genes in either case. These results suggested that an *FGFR3* p.R248H mutation is involved in the carcinogenesis of a subset of LCs.

A novel p.R248H mutation in the *FGFR3* gene was detected in two lung squamous cell carcinomas derived from Japanese patients with a smoking habit. The detection of the p.R248H mutation in two LCs suggests a recurrent mutation in LC. The p.R248C mutation occurred in the same codon as the p.R248H mutation and was previously shown to drive cellular transformation; additionally, the transformation was shown to be reversed by a small molecule FGFR inhibitor (17). Moreover, the p.R248C mutation was detected not only in LC, but also in urinary bladder cancer and multiple myeloma (10,11,23). Regarding the amino acid conversion from Arg to His, p.R175H and p.R273H in the *p53* gene are hotspot mutations and gain-of-function mutations (24,25), suggesting the effect of the amino acid exchange on carcinogenesis. In addition, the screening for non-acceptable polymorphisms (SNAP) program, which predicts the effect of single amino acid substitutions on protein function (http://www.rostlab.org/services/SNAP) (26), predicted that the *FGFR3* p.R248H mutation was non-neutral. Finally, in our qRT-PCR experiment, an increased FGFR3 expression was detected in both LCs containing a p.R248H mutation. Thus, the *FGFR3* p.R248H mutation may play an important role in the genesis and development of LCs. In the future, a precise functional investigation may aid in clarifying the role of the *FGFR3* p.R248H mutation.

There have been two previous reports investigating *FGFR3* mutations. Activating *FGFR3* mutations were detected at a frequency of 2.2% (4/178 squamous cell carcinomas) in one study (12) and 4.2% (2/48 squamous cell carcinomas) in another report (16). In the present study, the incidence of *FGFR3* mutation among squamous cell carcinomas derived from Japanese patients was 3.2%, although functional characterization of the mutant was not performed. These results suggested that *FGFR3* mutation is a recurrent event in lung squamous cell carcinomas in multiple populations.

FGFR3 fusion transcripts were previously found in one study at a frequency of 4.2% (2/48 squamous cell carcinomas) (16). On the other hand, no FGFR3 fusion transcripts were detected in our cases, suggesting that FGFR3 fusion may be rare in the Japanese population. However, since the number of analyzed squamous cell carcinoma cases in our study was relatively small (n=60) and FGFR3 may be fused with proteins other than TACC3 and BAIAP2L1, a future large study examining this issue is required to examine the incidence of FGFR3 fusion in LCs derived from Japanese patients.

In our *FGFR3* mutation-positive cases, the co-occurrence of *p53* mutation in one case and the co-occurrence of *PIK3CA* and *SOX2* amplification in the other case were observed. Both *p53* mutation and amplification of the *PIK3CA* and *SOX2* genes are frequent in lung squamous cell carcinoma (12,21,22). These results suggest that a combination of *FGFR3* mutation and such alterations may favor lung squamous cell carcinoma and *FGFR3* mutation is not mutually exclusive with such alterations in lung squamous cell carcinoma.

In conclusion, our *FGFR3* mutation-positive LCs in conjunction with previously detected *FGFR3* mutation-positive LCs suggested that an *FGFR3* mutation is involved in the carcinogenesis of a subset of LCs, especially lung squamous cell carcinomas, and may aid in elucidating the characteristics of *FGFR3* mutation-positive LCs in the future.

Acknowledgements

The authors wish to acknowledge Mr. T. Kamo (Hamamatsu University School of Medicine) for his technical assistance. The present study was supported in part by a grant-in-aid from the Ministry of Health, Labour and Welfare (21-1), a grant-in-aid from the Japan Society for the Promotion of Science (25460476), a grant-in-aid from the Ministry of Education, Culture, Sports, Science and Technology (221S0001), and the Smoking Research Foundation.

References

1. Soda M, Choi YL, Enomoto M, Takada S, Yamashita Y, Ishikawa S, Fujiwara S, Watanabe H, Kurashina K, Hatanaka H, Bando M, Ohno S, Ishikawa Y, Aburatani H, Niki T, Sohara Y, Sugiyama Y and Mano H: Identification of the transforming *EML4-ALK* fusion gene in non-small-cell lung cancer. Nature 448: 561-566, 2007.
2. Shinmura K, Kageyama S, Tao H, Bunai T, Suzuki M, Kamo T, Takamochi K, Suzuki K, Tanahashi M, Niwa H, Ogawa H and Sugimura H: EML4-ALK fusion transcripts, but no NPM-, TPM3-, CLTC-, ATIC-, or TFG-ALK fusion transcripts, in non-small cell lung carcinomas. Lung Cancer 61: 163-169, 2008.
3. Schmid K, Oehl N, Wrba F, Pirker R, Pirker C and Filipits M: *EGFR/KRAS/BRAF* mutations in primary lung adenocarcinomas and corresponding locoregional lymph node metastases. Clin Cancer Res 15: 4554-4560, 2009.
4. Kohno T, Ichikawa H, Totoki Y, Yasuda K, Hiramoto M, Nammo T, Sakamoto H, Tsuta K, Furuta K, Shimada Y, Iwakawa R, Ogiwara H, Oike T, Enari M, Schetter AJ, Okayama H, Haugen A, Skaug V, Chiku S, Yamanaka I, Arai Y, Watanabe S, Sekine I, Ogawa S, Harris CC, Tsuda H, Yoshida T, Yokota J and Shibata T: *KIF5B-RET* fusions in lung adenocarcinoma. Nat Med 18: 375-377, 2012.
5. Takeuchi K, Soda M, Togashi Y, Suzuki R, Sakata S, Hatano S, Asaka R, Hamanaka W, Ninomiya H, Uehara H, Lim Choi Y, Satoh Y, Okumura S, Nakagawa K, Mano H and Ishikawa Y: RET, ROS1 and ALK fusions in lung cancer. Nat Med 18: 378-381, 2012.
6. Lipson D, Capelletti M, Yelensky R, Otto G, Parker A, Jarosz M, Curran JA, Balasubramanian S, Bloom T, Brennan KW, Donahue A, Downing SR, Frampton GM, Garcia L, Juhn F, Mitchell KC, White E, White J, Zwirko Z, Peretz T, Nechushtan H, Soussan-Gutman L, Kim J, Sasaki H, Kim HR, Park SI, Ercan D, Sheehan CE, Ross JS, Cronin MT, Jänne PA and Stephens PJ: Identification of new *ALK* and *RET* gene fusions from colorectal and lung cancer biopsies. Nat Med 18: 382-384, 2012.
7. Matsuura S, Shinmura K, Kamo T, Igarashi H, Maruyama K, Tajima M, Ogawa H, Tanahashi M, Niwa H, Funai K, Kohno T, Suda T and Sugimura H: CD74-ROS1 fusion transcripts in resected non-small cell lung carcinoma. Oncol Rep 30: 1675-1680, 2013.
8. Oxnard GR, Binder A and Jänne PA: New targetable oncogenes in non-small-cell lung cancer. J Clin Oncol 31: 1097-1104, 2013.
9. Casaluce F, Sgambato A, Maione P, Rossi A, Ferrara C, Napolitano A, Palazzolo G, Ciardiello F and Gridelli C: ALK inhibitors: a new targeted therapy in the treatment of advanced NSCLC. Target Oncol 8: 55-67, 2013.
10. Cappellen D, De Oliveira C, Ricol D, de Medina S, Bourdin J, Sastre-Garau X, Chopin D, Thiery JP and Radvanyi F: Frequent activating mutations of FGFR3 in human bladder and cervix carcinomas. Nat Genet 23: 18-20, 1999.
11. Greulich H and Pollock PM: Targeting mutant fibroblast growth factor receptors in cancer. Trends Mol Med 17: 283-292, 2011.
12. Cancer Genome Atlas Research Network: Comprehensive genomic characterization of squamous cell lung cancers. Nature 489: 519-525, 2012.
13. Singh D, Chan JM, Zoppoli P, Niola F, Sullivan R, Castano A, Liu EM, Reichel J, Porrati P, Pellegatta S, Qiu K, Gao Z, Ceccarelli M, Riccardi R, Brat DJ, Guha A, Aldape K, Golfinos JG, Zagzag D, Mikkelsen T, Finocchiaro G, Lasorella A, Rabadan R and Iavarone A: Transforming fusions of *FGFR* and *TACC* genes in human glioblastoma. Science 337: 1231-1235, 2012.
14. Williams SV, Hurst CD and Knowles MA: Oncogenic FGFR3 gene fusions in bladder cancer. Hum Mol Genet 22: 795-803, 2013.
15. Wu YM, Su F, Kalyana-Sundaram S, Khazanov N, Ateeq B, Cao X, Lonigro RJ, Vats P, Wang R, Lin SF, Cheng AJ, Kunju LP, Siddiqui J, Tomlins SA, Wyngaard P, Sadis S, Roychowdhury S, Hussain MH, Feng FY, Zalupski MM, Talpaz M, Pienta KJ, Rhodes DR, Robinson DR and Chinnaiyan AM: Identification of targetable FGFR gene fusions in diverse cancers. Cancer Discov 3: 636-647, 2013.
16. Majewski IJ, Mittempergher L, Davidson NM, Bosma A, Willems SM, Horlings HM, de Rink I, Greger L, Hooijer GK, Peters D, Nederlof PM, Hofland I, de Jong J, Wesseling J, Kluin RJ, Brugman W, Kerkhoven R, Nieboer F, Roepman P, Broeks A, Muley TR, Jassem J, Niklinski J, van Zandwijk N, Brazma A, Oshlack A, van den Heuvel M and Bernards R: Identification of recurrent *FGFR3* fusion genes in lung cancer through kinome-centred RNA sequencing. J Pathol 230: 270-276, 2013.
17. Liao RG, Jung J, Tchaicha J, Wilkerson MD, Sivachenko A, Beauchamp EM, Liu Q, Pugh TJ, Pedamallu CS, Hayes DN, Gray NS, Getz G, Wong KK, Haddad RI, Meyerson M and Hammerman PS: Inhibitor-sensitive FGFR2 and FGFR3 mutations in lung squamous cell carcinoma. Cancer Res 73: 5195-5205, 2013.
18. Shinmura K, Goto M, Suzuki M, Tao H, Yamada H, Igarashi H, Matsuura S, Maeda M, Konno H, Matsuda T and Sugimura H: Reduced expression of MUTYH with suppressive activity against mutations caused by 8-hydroxyguanine is a novel predictor of a poor prognosis in human gastric cancer. J Pathol 225: 414-423, 2011.
19. Pao W and Girard N: New driver mutations in non-small-cell lung cancer. Lancet Oncol 12: 175-180, 2011.
20. Ulivi P, Romagnoli M, Chiadini E, Casoni GL, Capelli L, Gurioli C, Zoli W, Saragoni L, Dubini A, Tesei A, Amadori D and Poletti V: Assessment of *EGFR* and *K-ras* mutations in fixed and fresh specimens from transesophageal ultrasound-guided fine needle aspiration in non-small cell lung cancer patients. Int J Oncol 41: 147-152, 2012.
21. Mantripragada K and Khurshid H: Targeting genomic alterations in squamous cell lung cancer. Front Oncol 3: 195, 2013.
22. Pros E, Lantuejoul S, Sanchez-Verde L, Castillo SD, Bonastre E, Suarez-Gauthier A, Conde E, Cigudosa JC, Lopez-Rios F, Torres-Lanzas J, Castellví J, Ramon y Cajal S, Brambilla E and Sanchez-Cespedes M: Determining the profiles and parameters for gene amplification testing of growth factor receptors in lung cancer. Int J Cancer 133: 898-907, 2013.
23. Intini D, Baldini L, Fabris S, Lombardi L, Ciceri G, Maiolo AT and Neri A: Analysis of *FGFR3* gene mutations in multiple myeloma patients with t(4;14). Br J Haematol 114: 362-364, 2001.
24. Petitjean A, Mathe E, Kato S, Ishioka C, Tavtigian SV, Hainaut P and Olivier M: Impact of mutant p53 functional properties on *TP53* mutation patterns and tumor phenotype: lessons from recent developments in the IARC TP53 database. Hum Mutat 28: 622-629, 2007.
25. Yeudall WA, Vaughan CA, Miyazaki H, Ramamoorthy M, Choi MY, Chapman CG, Wang H, Black E, Bulysheva AA, Deb SP, Windle B and Deb S: Gain-of-function mutant p53 upregulates CXC chemokines and enhances cell migration. Carcinogenesis 33: 442-451, 2012.
26. Bromberg Y and Rost B: SNAP: predict effect of non-synonymous polymorphisms on function. Nucleic Acids Res 35: 3823-3835, 2007.

Natsume et al. Journal of Translational Medicine 2012, 10:97
http://www.translational-medicine.com/content/10/1/97

JOURNAL OF TRANSLATIONAL MEDICINE

RESEARCH Open Access

The *CRKL* gene encoding an adaptor protein is amplified, overexpressed, and a possible therapeutic target in gastric cancer

Hiroko Natsume[1], Kazuya Shinmura[1], Hong Tao[1], Hisaki Igarashi[1], Masaya Suzuki[1], Kiyoko Nagura[1], Masanori Goto[1], Hidetaka Yamada[1], Matsuyoshi Maeda[2], Hiroyuki Konno[3], Satoki Nakamura[4] and Haruhiko Sugimura[1*]

Abstract

Background: Genomic DNA amplification is a genetic factor involved in cancer, and some oncogenes, such as *ERBB2*, are highly amplified in gastric cancer. We searched for the possible amplification of other genes in gastric cancer.

Methods and Results: A genome-wide single nucleotide polymorphism microarray analysis was performed using three cell lines of differentiated gastric cancers, and 22 genes (including *ERBB2*) in five highly amplified chromosome regions (with a copy number of more than 6) were identified. Particular attention was paid to the *CRKL* gene, the product of which is an adaptor protein containing Src homology 2 and 3 (SH2/SH3) domains. An extremely high *CRKL* copy number was confirmed in the MKN74 gastric cancer cell line using fluorescence *in situ* hybridization (FISH), and a high level of CRKL expression was also observed in the cells. The RNA-interference-mediated knockdown of CRKL in MKN74 disclosed the ability of CRKL to upregulate gastric cell proliferation. An immunohistochemical analysis revealed that CRKL protein was overexpressed in 24.4% (88/360) of the primary gastric cancers that were analyzed. The *CRKL* copy number was also examined in 360 primary gastric cancers using a FISH analysis, and *CRKL* amplification was found to be associated with CRKL overexpression. Finally, we showed that MKN74 cells with *CRKL* amplification were responsive to the dual Src/BCR-ABL kinase inhibitor BMS354825, likely via the inhibition of CRKL phosphorylation, and that the proliferation of MKN74 cells was suppressed by treatment with a CRKL-targeting peptide.

Conclusion: These results suggested that CRKL protein is overexpressed in a subset of gastric cancers and is associated with *CRKL* amplification in gastric cancer. Furthermore, our results suggested that CRKL protein has the ability to regulate gastric cell proliferation and has the potential to serve as a molecular therapy target for gastric cancer.

Keywords: CRKL, Gastric cancer, Cell proliferation, Overexpression, Copy number amplification

Background

Although the overall incidence of gastric cancer is decreasing in many countries, the high incidence of gastric cancer remains a serious health problem, and gastric cancer continues to be the second-leading cause of cancer-related death worldwide [1,2]. Gastric carcinogenesis is a multi-step process in which environmental and genetic factors interact [1–8]. Among the genetic changes observed in cancerous cells, genomic DNA amplification is a well-known alteration that is involved in gastric cancer [4,5,7]. Amplification is often associated with increased expression levels of the genes contained in the amplified loci [5]. Oncogenes in gastric cancer, such as *MYC* (mapped to chromosome 8q24), *KRAS* (12p12), and *ERBB2* (17q12), are located in such amplified regions [4,5,7,9]. We considered the possibility that there exist genes whose amplification in gastric cancer has not been revealed to date. To uncover such novel gene alterations, we searched for highly amplified genes in

* Correspondence: hsugimur@hama-med.ac.jp
[1]Department of Tumor Pathology, Hamamatsu University School of Medicine, 1-20-1 Handayama, Higashi Ward, Hamamatsu, Shizuoka 431-3192, Japan
Full list of author information is available at the end of the article

gastric cancer using a genome-wide single nucleotide polymorphism (SNP) microarray analysis and found that the *CRKL* [*v-crk sarcoma virus CT10 oncogene homolog (avian)-like*] gene (22q11) is highly amplified in gastric cancer. The CRKL, a member of the CRK family of adapter proteins, consists of an NH2-terminal Src homology 2 (SH2) domain followed by two SH3 domains: SH3n and SH3c [10], and participates in signal transduction in response to growth factors, cytokines, and the oncogenic BCR-ABL fusion protein, resulting in cell proliferation, survival, adhesion, and migration [10,11]. We hypothesized that CRKL might play an important role in gastric carcinogenesis and investigated whether CRKL expression and the function of CRKL protein affect the regulation of cell proliferation in gastric cancer. We also investigated responsiveness of a gastric cancer cell line containing *CRKL* amplification to a kinase inhibitor, BMS354825, and a CRKL-targeting peptide.

Materials and Methods

Cell lines and surgical specimens

The gastric adenocarcinoma cell lines MKN7, MKN28, MKN74, and AGS were purchased from the Human Science Research Resource Bank (Osaka, Japan) or from American Type Culture Collection (Manassas, VA). Cells were cultured and grown in RPMI 1640 medium supplemented with 10% fetal bovine serum, penicillin (100 units/mL), and streptomycin (100 μg/mL) under a 5% CO_2 atmosphere at 37°C. Paraffin-embedded gastric tissues obtained from gastric cancer patients who underwent surgery at Toyohashi Municipal Hospital (Japan) were used for the immunohistochemical analysis. Gastric tissue samples obtained from gastric cancer patients who underwent surgery at Hamamatsu University Hospital (Japan) were used for the quantitative reverse-transcription (QRT)-polymerase chain reaction (PCR) analysis. The study design was approved by the Institutional Review Boards (IRBs).

Genome-wide SNP microarray

DNA (250 ng) was digested with *Nsp*I restriction enzyme (New England Biolabs, Hertfordshire, UK) and ligated to a universal adaptor sequence. The ligated DNA was PCR-amplified using primers complementary to the universal adaptors, and the PCR products were purified, quantified, and normalized. The products were then fragmented, end-labeled using terminal deoxynucleotidyl transferase, and hybridized to the Affymetrix GeneChip human mapping 250 K NspI arrays (Affymetrix Japan, Tokyo, Japan). After hybridization, the arrays were washed, stained using Affymetrix fluidics station 450, and scanned with a GeneChip Scanner 3000 7 G. Raw SNP call data were extracted using Affymetrix GeneChip Genotyping Analysis software (GTYPE) 4.1. The SNP microarray data were analyzed to determine the total copy number using the CNAG program, as previously described [12,13] (Figure 1).

WST-8 assay

Cell proliferation and viability were quantified using a Cell Counting Kit-8 (Dojindo, Kumamoto, Japan) according to the manufacturer's instructions [14]. The assay was based on the extracellular reduction of the tetrazolium salt WST-8 by NADH produced in the mitochondria of living cells. The cells were incubated with the WST-8 reagent for 1 hr at 37°C, and the absorbance was measured at 450 nm using an EL340I microplate reader (BIO-TEK Instruments, Winooski, VT) (Figure 2).

Immunohistochemistry

Tissue microarray (TMA) blocks were prepared as previously described [14-16]. TMA block sections were deparaffinized, rehydrated, and boiled in Tris-EDTA buffer (pH 9.0) for antigen retrieval. Endogenous peroxidase activity was blocked by incubation in a hydrogen peroxide solution. Next, the sections were incubated with a rabbit anti-CRKL monoclonal antibody (Y243; Abcam, Cambridge, UK). The antigen-antibody complex was visualized using Histofine Simple Stain Max-Po (Multi) (Nichirei, Tokyo, Japan) and 3,3'-diaminobenzidine tetrahydrochloride. Counterstaining was performed using hematoxylin. The intensity values of the cells were determined using a 4-point scale according to the color of the cell cytoplasm after CRKL immunostaining as follows: 0, blue; 1, blue-brown; 2, light brown; and 3, brown. The percentage of cells with each intensity value was then multiplied by the intensity value, as described previously [14]. The scores obtained for CRKL immunostaining were classified as either a low expression level (0–0.99) or a high expression level (1.00–3.00) (Figure 3).

DNA fluorescence *in situ* hybridization (FISH)

FISH was performed as previously described [16-19]. Tissue slides were hybridized with a Spectrum Orange-labeled BAC clone (RP11-801O20 and RP11-1058B20) for the *CRKL* locus (Advanced GenoTechs Co., Tsukuba, Japan) and a Spectrum Green-labeled control probe for the near centromere locus on chromosome 22 (BAC clone: RP11-232E17). 4',6-Diamidino-2-phenylindole (DAPI) (Vector Laboratories, Burlingame, CA) was used for nuclear staining (Figure 3).

MTT assay and direct cell counting

In the experiment involving treatment with the CRKL-targeting peptide, an MTT assay was performed to assess cell viability in Figure 4G. The cells were cultured with the indicated concentration of CRKL-targeting peptide or dimethyl sulfoxide (DMSO) at 37°C for 72 h, and 3-(4,5-dimethylthiazol-2-yl)-2,5-diphenyltetrazolium

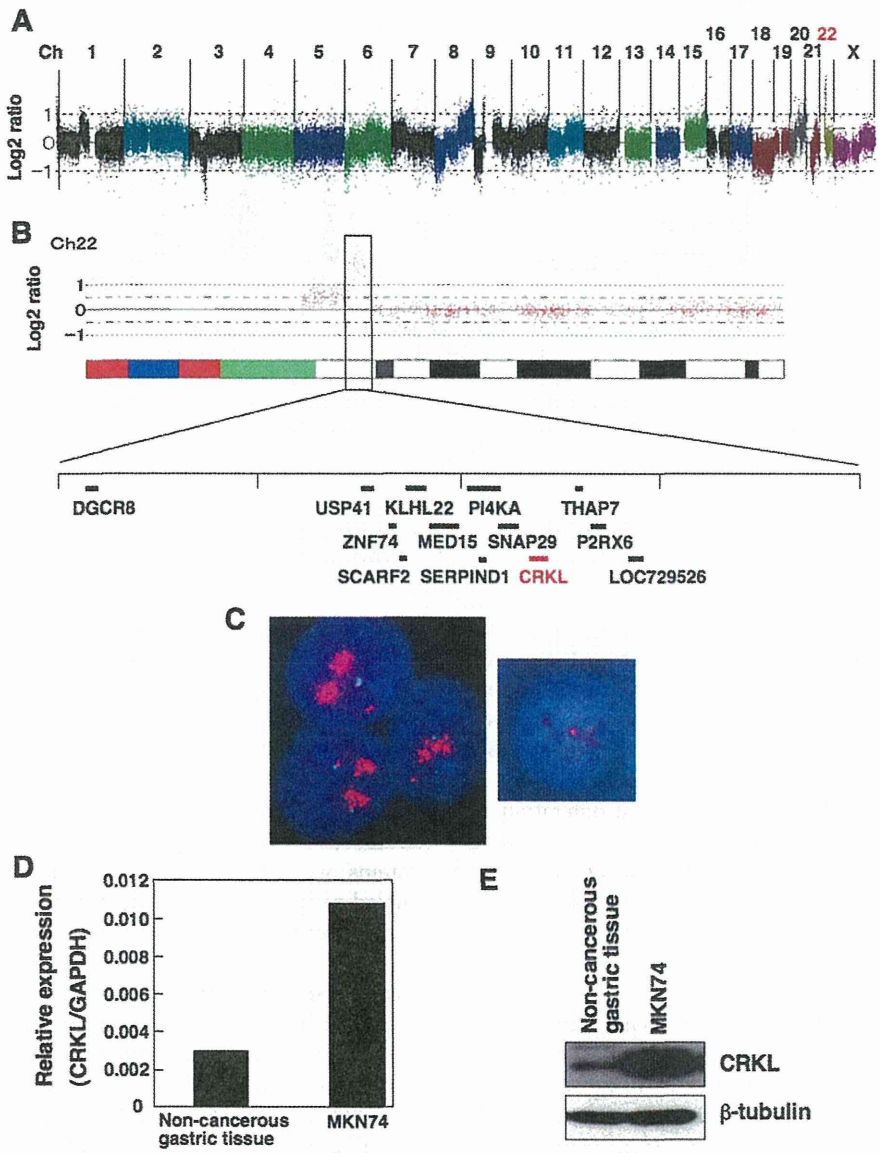

Figure 1 Identification of highly amplified chromosome regions containing the *CRKL* gene and the detection of CRKL overexpression in gastric cancer. (A) Genome-wide detection of copy number alterations using a high-density SNP microarray in the MKN74 gastric cancer cell line. The copy number status for the whole genome of MKN74 is shown. DNA (250 ng) was analyzed using an Affymetrix GeneChip 250 K NspI array, and the total copy numbers were determined by analyzing the microarray data using the CNAG program. The chromosome number is shown above the panel. Chromosome 22 is highlighted in red. **(B)** The copy number status of chromosome 22 of the MKN74 cells is shown. A highly amplified region of chromosome 22 is enlarged, and the genes located in this region are indicated. The *CRKL* gene is highlighted in red. **(C)** Detection of *CRKL* amplification in MKN74 cells using a FISH analysis. The left panel shows the *CRKL* signal (red) in MKN74 cells, while the right panel shows the *CRKL* (red) in non-cancerous gastric tissue cells. An extreme increase in the *CRKL* copy number was observed in the MKN74 cells, while a normal copy number (2) was seen in non-cancerous cells. Nuclei are stained with DAPI. **(D)** Detection of the increased expression of CRKL mRNA transcript in MKN74 cells using real-time QRT-PCR analysis. The amounts of CRKL transcripts normalized to the amount of GAPDH transcripts are shown in the graph. The average expression level of eight normal gastric mucosa samples was measured as a control. **(E)** Detection of the increased expression of CRKL protein in MKN74 cells using a western blot analysis. The expression of CRKL was examined using anti-CRKL monoclonal antibody (Y244; 1:500 dilution), horseradish peroxidase-coupled secondary antibody (1:5,000 dilution), and enhanced chemiluminescence detection reagents. The expression of β-tubulin protein was analyzed as an internal control.

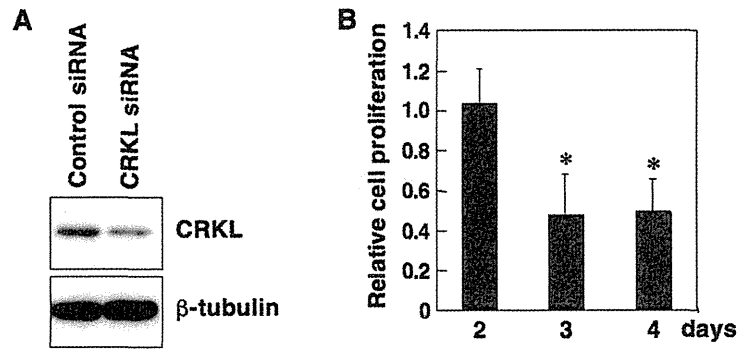

Figure 2 Ability of CRKL to regulate cell proliferation in the MKN74 gastric cancer cell line. (A) siRNA knockdown for CRKL in MKN74 cells with *CRKL* amplification. Cells were reverse-transfected with the siRNA oligonucleotides (20 nM) using HiPerFect Transfection Reagent, and 8×10^5 cells were seeded in 60 mm-dishes with 4 ml media. The expression of CRKL was examined 4 days after the reverse transfection of CRKL siRNA or negative control siRNA using a western blot analysis with anti-CRKL monoclonal antibody (Y244; 1:500 dilution). The level of CRKL protein expression was decreased in CRKL siRNA-transfected cells, compared with mock-transfected cells. The expression of β-tubulin protein was analyzed as an internal control. **(B)** Decrease in the proliferation of MKN74 cells transfected with siRNA for CRKL. Cells were reverse-transfected with the siRNA oligonucleotides (20 nM), and 1.5×10^4 cells were seeded in 96-well microplates containing 100 μL of media. After the reverse transfection of CRKL siRNA or negative control siRNA, the number of viable cells was counted by measuring the reduction in the tetrazolium monosodium salt WST-8. The cell number of CRKL siRNA-transfected cells relative to that of mock-transfected cells is shown. Values are the mean ± standard deviation of three independent experiments. *P*-values were calculated using the *t*-test, and * indicates a statistical significance.

bromide (MTT) solution (Sigma-Aldrich, St. Louis, MO) was then added at a final concentration of 0.25 mg/mL. After incubation at 37°C for 4 h, absorbance was measured at a wavelength of 570 nm using a microplate reader. Cells grown in complete medium with DMSO alone were used as controls. The final concentration of DMSO was set to 0.2%. To assess cell proliferation in Figure 4H, the cells were cultured with CRKL targeting peptide or DMSO at 37°C for 72 h. Cell proliferation was measured by directly counting the cells using a hemocytometer, as described previously [20].

QRT-PCR

Total RNA was extracted using Isogen (Nippongene, Tokyo, Japan) or an RNeasy Plus mini kit (Qiagen, Valencia, CA) and converted to cDNA using the SuperScript First-Strand Synthesis System (Invitrogen, Carlsbad, CA). Real-time QRT-PCR was performed using the cDNA and Fast SYBR Green Master Mix (Applied Biosystems, Foster City, CA) on a StepOne Real-Time PCR system (Applied Biosystems). The following PCR primers were used: 5'-CAA CCT GCC TAC AGC AGA AGA TAA-3' and 5'-CGG CAT CAT TCC CAG GAA-3' for the CRKL transcript, and 5'-GGT GGT CTC CTC TGA CTT CAA CA-3' and 5'-GTT GCT GTA GCC AAA TTC GTT GT-3' for the transcript of a housekeeping gene, *GAPDH*. The relative amounts of CRKL transcript were normalized to those of the GAPDH transcript.

Western blot analysis

Cells were lysed, and the protein concentration was quantified using a BCA protein assay kit (Pierce, Rockford, IL). The proteins were electrophoresed and transferred to a PVDF membrane (GE Healthcare Bio Science, Piscataway, NJ). After blocking with non-fat milk or Blocking One-P (Nakalai Tesque, Kyoto, Japan), the membrane was incubated with rabbit anti-CRKL monoclonal antibody (Y244; Abcam), rabbit anti-phospho CRKL polyclonal antibody (Y207; Cell Signaling, Beverly, MA), or mouse anti-β-tubulin (2-28-33, Sigma-Aldrich). The immunoreactive proteins were visualized using horseradish peroxidase-coupled secondary antibody and enhanced chemiluminescence detection reagents (GE Healthcare Bio Science) [21].

Small interfering RNA (siRNA) knockdown

A stealth siRNA duplex oligonucleotide (Invitrogen) was used for siRNA knockdown. The following CRKL sequence was used: 5'-UCG UGA AAG UCA CAA GGA UGA AUA U-3'. A low GC Duplex #2 (Invitrogen) was used as a negative control. MKN74 cells were reverse-transfected with the siRNA oligonucleotides (20 nM) using HiPerFect Transfection Reagent (Qiagen), according to the manufacturer's instructions.

BMS354825 and AMN107 treatment

BMS354825, a dual Src/BCR-ABL kinase inhibitor, was kindly provided by Bristol-Myers Squibb (New York, NY), and AMN107, a highly selective BCR-ABL kinase inhibitor, was kindly provided by Novartis Pharmaceuticals (Basel, Switzerland) [22-25]. Stock solutions (10 mM) of BMS354825 and AMN107 were prepared in DMSO. The cells were incubated with BMS354825 or AMN107 at a final concentration of 0.01 to 1.0 μM for 72 h. The final concentration of DMSO was set to 0.1%.

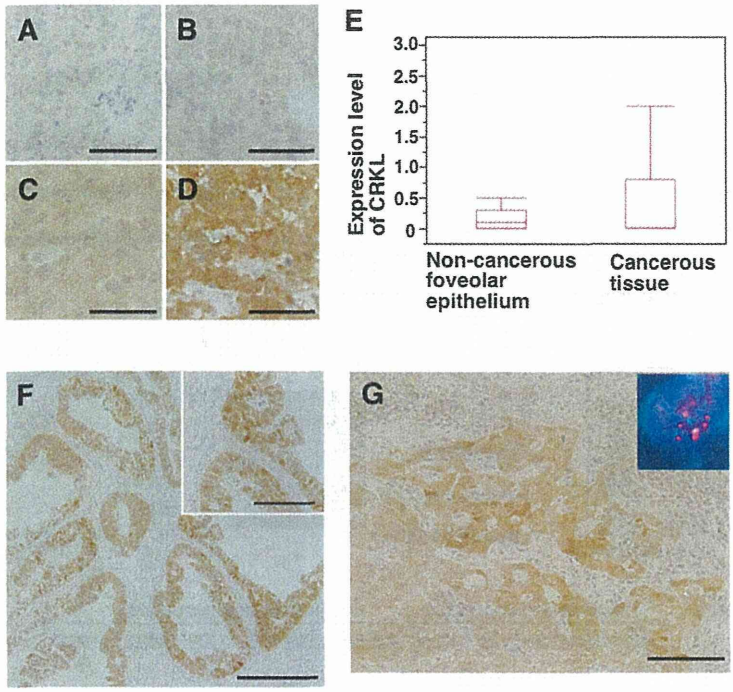

Figure 3 Immunohistochemical detection of CRKL protein in primary gastric cancer. TMA block sections were subjected to an immunohistochemical analysis using anti-CRKL monoclonal antibody (Y243; 1:100 dilution), Histofine Simple Stain Max-Po (Multi), and 3,3'-diaminobenzidine tetrahydrochloride. Intensity values of 0, 1, 2, and 3 are shown in **(A)**, **(B)**, **(C)**, and **(D)**, respectively. Bar = 50 μm. **(E)** Box-plot analysis of CRKL protein expression in gastric tissue. A statistically significant difference in the CRKL expression level was detected between non-cancerous gastric foveolar epithelium ($n = 41$) and gastric cancerous tissue ($n = 360$). **(F)** Representative result of the CRKL immunohistochemical analysis. A gastric cancer with a high CRKL expression level is shown. Bar = 500 μm. The inset is a magnified image. Bar = 50 μm. **(G)** Representative gastric cancer case showing both a high CRKL expression level and *CRKL* gene amplification. The high CRKL expression level (value = 2.6) was detected using an immunohistochemical analysis. Bar = 100 μm. The inset shows the amplification of *CRKL* (red) in the cancer cells. The *CRKL* signal (red) and the control signal for chromosome 22 (green) were detected using a FISH analysis. Nuclei are stained with DAPI.

Preparation of CRKL targeting peptide

In this study, we used the peptides, which has been reported to be disrupted complexes between BCR-ABL and CRKL depend on the SH3 domain of CRKL in CML cells [26]. Peptides used in the experiments are followed: CRKL-targeting peptide; KKW KMR RNP FWI KIQ RC – CGI RVV DNS PPP ALP PKR RRS APS PTR V, control peptide; KKW KMR RNP FWI KIQ RC – CGI RVV DNS PPG ALG PLL RRS APS PTR V. The KKW KMR RNP FWI KIQ RC was the shuttle tag sequence performing a receptor-independent cell entry. The chimeric peptide was synthesized and purified by using reverse-phase high performance liquid chromatography (HPLC) (Toray Research Center, Otsu, Japan). Peptide stocks were prepared in DMSO and stored in aliquots at -80°C.

Statistical analysis

The statistical analysis was performed using an unpaired *t*-test, chi-square test, or Dunnett's test. JMP version 7.0.1 software (SAS Institute, Cary, NC) was used for the analyses. *P* values less than 0.05 were considered statistically significant.

Results

Identification of *CRKL* amplification in gastric cancer

To search for highly amplified genes in gastric adenocarcinoma, we adopted a genome-wide high-resolution SNP microarray approach in three cell lines of differentiated gastric adenocarcinoma: MKN7, MKN28, and MKN74. Genotype calls were obtained at more than 95% of the 262,264 SNP sites on the array, meaning that the SNP microarray analysis had been performed properly. The SNP microarray data were then used to determine the chromosomal copy number using the CNAG program (Figures 1A and 1B). Five highly amplified regions with a copy number of more than 6 (9p13, 17q12-q21, 19q12, 19q13, and 22q11) were identified, as shown in Table 1. These regions contained various kinds of genes, a total of 22 genes (Table 1). Among them, we decided to focus on the *CRKL* gene at chromosome 22q11.21, the product

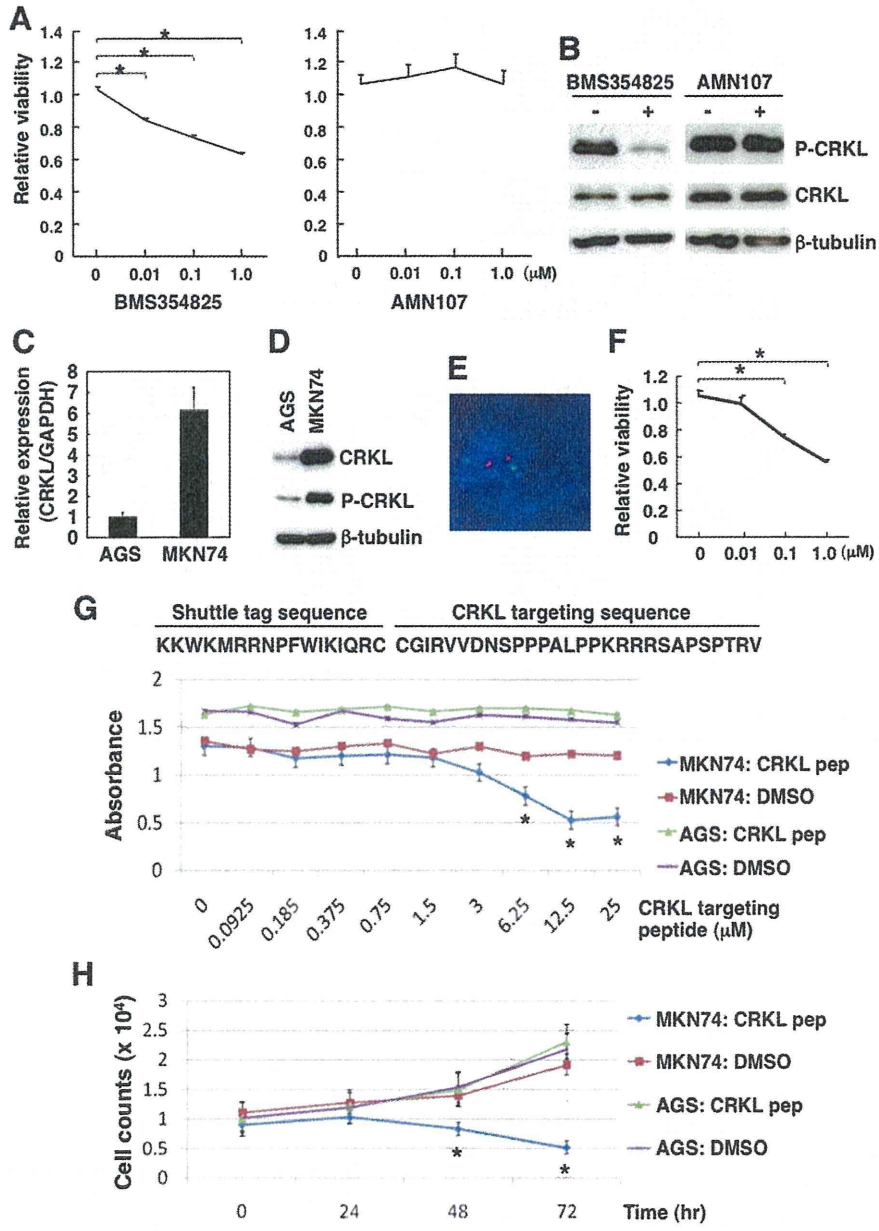

Figure 4 (See legend on next page)

of which is an SH2 and SH3 domain-containing adaptor protein that shares homology with the CRK oncoprotein, because CRKL is a known substrate of BCR-ABL kinase in Philadelphia chromosome-positive leukemia [27,28] and its role in gastric cancer has not been previously analyzed. To confirm that *CRKL* gene amplification was detectable in the MKN74 cell line, we performed a FISH analysis using a probe specific for *CRKL*. As expected, an extreme increase in the *CRKL* copy number was detected in the MKN74 cells using a FISH analysis (Figure 1C). When the level of CRKL mRNA expression was examined in MKN74 cells using a real-time QRT-PCR analysis, the level was much higher than that in non-cancerous gastric tissue (Figure 1D). Moreover, a western blot analysis showed that the level of CRKL protein expression was higher in MKN74 cells than in non-cancerous gastric tissue (Figure 1E). These results suggested that the *CRKL* gene is highly amplified and that CRKL is overexpressed in a subset of gastric cancer cell lines.

(See figure on previous page)

Figure 4 Responses of the MKN74 gastric cancer cell line with *CRKL* amplification to treatment with BMS354825 (a dual Src/BCR-ABL kinase inhibitor) and CRKL-targeting peptide. (A) Viability of MKN74 cells treated with BMS354825 but not those treated with AMN107 (a highly selective BCR-ABL kinase inhibitor) is decreased. The cells were seeded in 96-well microplates at a density of 1×10^4 per well; after 24 h, the drug (0.01–1.0 μM) or 0.1% DMSO solution was added. Viability was examined in the MKN74 cells after 72 h of treatment at the indicated concentration using WST-8 reagent. The number of viable cells after treatment with each inhibitor was normalized to the number of viable cells without treatment, and the relative viability is shown in the graph. Values are the mean ± standard error. *P* values were calculated using the Dunnett's multiple comparison test, and * indicates a statistically significant decrease. **(B)** Effective inhibition of CRKL phosphorylation in MKN74 cells treated with BMS354825. Cells were treated with each inhibitor (DMSO only or 0.01 μM of drug) for 90 min, and the expression of CRKL protein was examined using a western blot analysis with anti-phospho CRKL polyclonal antibody (Y207; 1:1,000 dilution) or anti-CRKL monoclonal antibody (Y244; 1:500 dilution). The expression of β-tubulin protein was analyzed as an internal control. **(C)** Comparison of CRKL mRNA transcripts between AGS and MKN74 cells using real-time QRT-PCR analysis. The amounts of CRKL transcripts normalized to the amount of GAPDH transcripts are shown in the graph. **(D)** Comparison of expression of CRKL protein between AGS and MKN74 cells using a western blot analysis. The expression of CRKL was examined using the primary antibodies shown in (B). The expression of β-tubulin protein was analyzed as an internal control. **(E)** Detection of *CRKL* gene copy number in AGS cells using a FISH analysis. The *CRKL* signal is red, and the control signal for chromosome 22 is green. Nuclei are stained with DAPI. **(F)** Viability of AGS cells decreased after BMS354825 treatment. Viability was examined as described in (A). Values are the mean ± standard error. *P* values were calculated using a *t*-test, and * indicates a statistically significant decrease. **(G)** MKN74 cells with *CRKL* amplification and AGS cells without *CRKL* amplification were seeded in 96-well microplates at a density of 1×10^4 per well. 24 h after seeding, cells were treated with CRKL-targeting peptide (0.0925–25 μM) or 0.2% DMSO solution at the indicated concentration. The sequence of the CRKL-targeting peptide that was used is shown above the graph. After 72 h of incubation, viability was determined using an MTT assay. The results are presented as the mean ± standard deviation of three independent experiments. *P* values were calculated using a *t*-test, and * indicates a statistically significant difference between the cells treated with CRKL-targeting peptide and those treated with DMSO. **(H)** Cell proliferation of MKN74 and AGS cells treated with CRKL-targeting peptide (6.25 μM) or DMSO as measured by counting cells using a hemocytometer. Cells (1×10^4) were seeded in 24-well plates and treated with CRKL-targeting peptide or DMSO. The cell counting was performed every 24 h for 3 days. Data are shown as the mean ± standard deviation of three independent experiments. *P* values were calculated using a *t*-test, and * indicates a statistically significant difference between the cells treated with CRKL-targeting peptide and those treated with DMSO.

Ability of CRKL to control gastric cell proliferation

To explore the functional significance of *CRKL* amplification in gastric cancer, we attempted to examine the effect of overexpressed CRKL on gastric cell proliferation. For this purpose, we prepared MKN74 cells with distinct CRKL expression levels using the siRNA knockdown of CRKL expression. CRKL-specific siRNA transfection effectively decreased the level of CRKL protein expression in MKN74 cells by approximately 70% of the levels observed in negative control siRNA-transfected cells (Figure 2A). A cell proliferation assay showed that the number of CRKL siRNA-transfected MKN74 cells was significantly lower at 3 and 4 days after transfection than the number of negative control siRNA-transfected cells (Figure 2B), meaning that CRKL has the ability to upregulate cell proliferation.

Table 1 Detection of chromosomal regions with a high copy number (more than 6) in the gastric cancer cell lines MKN7, MKN28, and MKN74 using a genome-wide SNP microarray analysis

Chromosomal regions[a]	Genes with a high copy number in the region
9p13	*PAX5*
17q12-q21	*FBXL20, MED1, PERLD1, ERBB2, IKZF3, ZPBP2*
19q12	*CCNE1*
19q13	*CD22*
22q11	*DGCR8, USP41, ZNF74, SCARF2, KLHL22, MED15, PI4KA, SERPIND1, SNAP29, CRKL, THAP7, P2RX6, LOC729526*

[a] If more than four consecutive SNP probes with a copy number of more than six were detected in either of the three cell lines, the chromosomal region was regarded as being a "highly amplified region" and was listed in this table.

Overexpression of CRKL protein in gastric cancer

Next, we investigated the expression status of CRKL protein in primary gastric cancer using an immunohistochemical analysis with anti-CRKL monoclonal antibody (Y243). CRKL was mainly observed in the cytoplasm, consistent with previous reports [29]. When we compared the level of CRKL expression between non-cancerous gastric foveolar epithelium ($n = 41$) and gastric cancer ($n = 360$), the level of CRKL expression in gastric cancer (mean ± standard deviation = 0.42 ± 0.63) was significantly higher than that in non-cancerous tissue (0.20 ± 0.26) ($P = 0.032$) (Figures 3A-3E). When an expression level of 1.00, which corresponds to a value 5-fold of the mean expression level in non-cancerous gastric foveolar epithelium, was used as a cutoff value for the expression status in gastric cancer (i.e., low expression group, 0–0.99; high expression group, 1.00–3.00), 88 (24.4%) of the 360 primary gastric cancers were included in the high expression group (Figure 3F). To examine whether CRKL overexpression is associated with *CRKL* amplification in gastric cancer, we performed a FISH analysis for the *CRKL* gene in the 360 primary gastric cancers and compared the prevalence of *CRKL* amplification between the low expression group and the high expression group. As

expected, the percentage of gastric cancer cells with *CRKL* amplification was significantly higher in the high expression group (9.1%; 8/88 cases) than in the low expression group (2.2%; 6/272 cases) ($P = 0.028$, chi-square test). This result suggests that *CRKL* amplification contributes to CRKL overexpression in primary gastric cancer. We further investigated whether the levels of CRKL expression is associated with clinicopathological features in primary gastric cancer patients, the high CRKL expression was observed significantly more often in male and differentiated-type gastric cancer (Table 2). These results suggested that CRKL protein is overexpressed partly due to *CRKL* amplification in a subset of primary gastric cancers and is associated with the gender and histopathology.

Decrease in the viability of CRKL-expressing MKN74 cells treated with BMS354825

Finally, we tested the possibility of using CRKL as a therapeutic target in MKN74 cells with *CRKL* amplification. Since Philadelphia chromosome-positive leukemia expressing BCR-ABL is responsive to BMS354825 (a dual Src/BCR-ABL kinase inhibitor) and AMN107 (a highly selective BCR-ABL kinase inhibitor) [22,24], we checked the response of MKN74 cells to both inhibitors. Cell viability was significantly decreased in BMS354825-treated (0.01–1.0 μM) MKN74 cells, compared with cells treated with the solvent only, while it was not significantly decreased in AMN107-treated cells (Figure 4A). When the status of CRKL phosphorylation was examined in the MKN74 cells using western blot analysis with an anti-phospho CRKL antibody, CRKL phosphorylation was found to be inhibited more effectively by BMS354825 than by AMN107 (Figure 4B). These results suggested that BMS354825 has the potential to suppress the viability of MKN74 cells expressing CRKL, likely via the inhibition of CRKL phosphorylation.

To further characterize the role of CRKL in the BMS354825-induced suppression of MKN74 cell viability, we examined the effect of BMS354825 on gastric cancer cells without *CRKL* amplification. Since the AGS gastric cancer cell line had lower CRKL mRNA and CRKL protein expression levels than MKN74 cells (Figures 4C and D) and had a normal *CRKL* genomic copy number (Figure 4E), these cells were treated with BMS354825. Unexpectedly, the viability of the BMS354825-treated (0.1–1.0 μM) AGS cells decreased significantly (Figure 4F). Moreover, although the IC_{50} value (inhibitory concentration producing a 50% response) for BMS354825 was slightly higher in AGS cells than in MKN74 cells, the values were not much different between AGS and MKN74 cells (data not shown). These results suggest that BMS354825 has the potential to suppress the viability of AGS cells, likely via a CRKL-independent pathway.

Table 2 Association between CRKL expression and clinicopathological factors in 360 patients with primary gastric cancer

		CRKL expression level		
Factor	Patient	Low ($n = 272$)	High ($n = 88$)	*P*
Age				
Year, mean ± SD[a]	62.0 ± 11.2	61.7 ± 11.7	62.9 ± 11.4	0.3936[b]
(range)	(29–86)	(29–86)	(31–85)	
Gender				
Male	255	182 (66.9%)	73 (83.0%)	0.0028[c]
Female	105	90 (33.1%)	15 (17.0%)	
Histological type				
Differentiated	172	118 (43.4%)	54 (61.4%)	0.0033[c]
Undifferentiated	188	154 (56.6%)	34 (38.6%)	
pT stage				
pT1	143	103 (37.9%)	40 (45.5%)	0.2082[c]
pT2-pT4	217	169 (62.1%)	48 (54.5%)	

[a] SD, standard deviation. [b] *t*-test. [c] Chi-square test.

Decrease in the viability/proliferation of CRKL-expressing MKN74 cells treated with a CRKL-targeting peptide

We then planned to use a more specific inhibitor of CRKL and examined the response of MKN74 and AGS cells to a CRKL-targeting peptide [26]. Cell viability decreased significantly in MKN74 cells treated with the CRKL-targeting peptide (6.25–25 μM), compared with DMSO (solvent)-treated cells, but a similar decrease was not found in AGS gastric cancer cells without *CRKL* amplification (Figure 4G). When cell proliferation was compared after treatment with 6.25 μM of the CRKL-targeting peptide, the cell proliferation was significantly suppressed in MKN74 cells treated with the peptide, compared with DMSO-treated MKN74 cells, but no inhibition of cell proliferation was seen in the AGS cells (Figure 4H). Control peptide had no effect on the gastric cancer cell proliferation. These results suggested that the CRKL-targeting peptide has the potential to suppress the viability/proliferation of gastric cells exhibiting *CRKL* amplification, but not of gastric cells that do not exhibit *CRKL* amplification.

Discussion

Through a genome-wide SNP microarray analysis performed in this study, the *CRKL* gene was identified as a highly amplified gene in gastric cancer. An increase in the copy number was confirmed in MKN74 gastric cancer cells with *CRKL* amplification using a FISH analysis, and a high CRKL expression level was also observed in these cells. The ability of CRKL to upregulate cell proliferation was shown in MKN74 cells by comparing the cell proliferation rate between CRKL siRNA-transfected cells and negative control siRNA-transfected cells. CRKL

protein was overexpressed in 24.4% of the primary gastric cancers, and its level in the gastric cancer was associated with the gender and histopathology. *CRKL* amplification was more frequently found in primary gastric cancers with high CRKL protein expression levels than in those with low CRKL expression levels. Finally, we showed that MKN74 cells with *CRKL* amplification were responsive to the kinase inhibitor BMS354825, likely via the inhibition of CRKL phosphorylation, and a CRKL-targeting peptide. Our current findings suggest that CRKL has an important role in the development of a subset of gastric cancers and has the potential to be a molecular therapy target for gastric cancer.

CRKL is an adaptor cell signaling protein that contains an SH2 domain and two tandem SH3 domains, both of which mediate protein-protein interactions [27,28,30]. CRKL is well known as a surrogate substrate of BCR-ABL kinase in chronic myeloid leukemia and acute lymphoblastic leukemia [11,27,28], and intensive studies of CRKL in Philadelphia chromosome-positive leukemia have been performed. However, only one paper by Kim *et al.* [31] has reported the CRKL status in gastric cancer. They revealed that the expression of CRKL mRNA in a cancer cell line was stimulated by proteins released by *Helicobacter pylori*, although the underlying mechanism was not resolved and the *CRKL* genomic copy number was not analyzed. Our genome-wide SNP microarray analysis successfully revealed, for the first time, that the *CRKL* gene is highly amplified in a subset of gastric cancers. We also showed that the CRKL protein can upregulate cell proliferation using the RNA-interference-mediated knockdown of CRKL in a gastric cancer cell line with *CRKL* amplification. Thus, CRKL overexpression arising from genomic amplification likely contributes to the aggressiveness of gastric cancer.

Recent progress in the development of molecular cancer therapy has revealed new molecular-targeting drugs, such as EGFR-targeting drug ZD1839 (Iressa) and HER2-targeting anti-HER2 monoclonal antibody trastuzumab (Herceptin), to be potent therapies for specific cancers [32-34]. In this study, BMS354825, a dual inhibitor for Src and BCR-ABL kinases, but not AMN107, a BCR-ABL specific inhibitor, showed an inhibitory effect on the survival of MKN74 cells with *CRKL* amplification. A decrease in CRKL phosphorylation through the inhibition of a currently unknown Src kinase seems to be one of the main mechanisms of BMS354825-mediated cytotoxicity in MKN74 cells. BMS354825 is currently being studied clinically in colorectal cancer, prostate cancer, breast cancer, lung cancer, and Philadelphia chromosome-positive leukemia [22,23,35]. Our results suggest that the CRKL protein may be a target of BMS354825-mediated therapy for a subset of gastric cancers. In our analyses, BMS354825 suppressed the viability of AGS cells without *CRKL* amplification as well as the viability of MKN74 cells with *CRKL* amplification, suggesting that a CRKL-independent pathway, which has been previously implicated [36], may also be involved in the BMS354825-mediated cytotoxicity seen in gastric cancers. We also presented the usefulness of a CRKL-targeting peptide for suppressing the proliferation of MKN74 cells with *CRKL* amplification. Our results should contribute to the establishment of CRKL-targeting therapy for a subset of gastric cancers in the future.

In the present study, a genome-wide, high-resolution SNP microarray analysis was successfully performed and five highly amplified chromosome regions containing 22 genes were identified in gastric cancers, as listed in Table 1. Although the *ERBB2* gene, a well-known oncogene that is often amplified in gastric cancer [4], was included in this list, the roles of the most of the genes in the Table have not been studied in gastric cancer. Further investigation of these roles is needed in the future.

Conclusion

We conclude that CRKL protein is overexpressed in a subset of gastric cancers and is associated with *CRKL* amplification in gastric cancer. Furthermore, we conclude that CRKL protein has the ability to regulate gastric cell proliferation and has the potential to serve as a molecular therapy target for gastric cancer.

Abbreviations

DAPI: 4',6-diamidino-2-phenylindole; DMSO: Dimethyl sulfoxide; FISH: Fluorescence *in situ* hybridization; QRT-PCR: Quantitative reverse-transcription-polymerase chain reaction; SNP: Single nucleotide polymorphism; siRNA: Small interfering RNA; TMA: Tissue microarray; SH2/SH3: Src homology 2 and 3.

Competing interests

The authors declare that they have no competing interests.

Acknowledgements

We greatly appreciate the critical reading of the manuscript by Prof.Shinya Tanaka at Hokkaido University. This work was supported by grants from the Ministry of Health, Labour and Welfare (21-1), the Japan Society for the Promotion of Science (21790383, 22590356, and 22790378), the Ministry of Education, Culture, Sports, Science and Technology (20014007 and 221 S0001), and the Smoking Research Foundation.

Author details

[1]Department of Tumor Pathology, Hamamatsu University School of Medicine, 1-20-1 Handayama, Higashi Ward, Hamamatsu, Shizuoka 431-3192, Japan. [2]Department of Pathology, Toyohashi Municipal Hospital, 50 Hachiken Nishi, Aotake-cho, Toyohashi, Aichi 441-8570, Japan. [3]Second Department of Surgery, Hamamatsu University School of Medicine, 1-20-1 Handayama, Higashi Ward, Hamamatsu, Shizuoka 431-3192, Japan. [4]Third Department of Internal Medicine, Hamamatsu University School of Medicine, 1-20-1 Handayama, Higashi Ward, Hamamatsu, Shizuoka 431-3192, Japan.

Authors' contributions

HN performed the experiments and wrote the paper draft. KS and SN interpreted the data and revised the paper. HT, HI, MS, KN, MG, SN,

and HY performed a part of the experiments. MM and HK provided tissue samples. SN performed a part of the experiments and was involved in the experimental design. HS conceived the research, designed the experiment, and revised the paper. All authors have read and approved the manuscript.

Received: 22 December 2011 Accepted: 16 May 2012
Published: 16 May 2012

References

1. Crew KD, Neugut AI: **Epidemiology of gastric cancer.** *World J Gastroenterol* 2006, **12**:354–362.
2. Hohenberger P, Gretschel S: **Gastric cancer.** *Lancet* 2003, **362**:305–315.
3. Shinmura K, Kohno T, Takahashi M, Sasaki A, Ochiai A, Guilford P, Hunter A, Reeve AE, Sugimura H, Yamaguchi N, Yokota J: **Familial gastric cancer: clinicopathological characteristics, RER phenotype and germline *p53* and *E-cadherin* mutations.** *Carcinogenesis* 1999, **20**:1127–1131.
4. Tahara E: **Genetic pathways of two types of gastric cancer.** *IARC Sci Publ* 2004, **157**:327–349.
5. Yang S, Jeung HC, Jeong HJ, Choi YH, Kim JE, Jung JJ, Rha SY, Yang WI, Chung HC: **Identification of genes with correlated patterns of variations in DNA copy number and gene expression level in gastric cancer.** *Genomics* 2007, **89**:451–459.
6. Study Group of Millennium Genome Project for Cancer, Sakamoto H, Yoshimura K, Saeki N, Katai H, Shimoda T, Matsuno Y, Saito D, Sugimura H, Tanioka F, Kato S, Matsukura N, Matsuda N, Nakamura T, Hyodo I, Nishina T, Yasui W, Hirose H, Hayashi M, Toshiro E, Ohnami S, Sekine A, Sato Y, Totsuka H, Ando M, Takemura R, Takahashi Y, Ohdaira M, Aoki K, Honmyo I, Chiku S, Aoyagi K, Sasaki H, Ohnami S, Yanagihara K, Yoon KA, Kook MC, Lee YS, Park SR, Kim CG, Choi IJ, Yoshida T, Nakamura Y, Hirohashi S: **Genetic variation in *PSCA* is associated with susceptibility to diffuse-type gastric cancer.** *Nat Genet* 2008, **40**:730–740.
7. Calcagno DQ, Leal MF, Assumpcao PP, Smith MA, Burbano RR: ***MYC* and gastric adenocarcinoma carcinogenesis.** *World J Gastroenterol* 2008, **14**:5962–5968.
8. Shin VY, Jin H, Ng EK, Cheng AS, Chong WW, Wong CY, Leung WK, Sung JJ, Chu KM: **NF-κB targets miR-16 and miR-21 in gastric cancer: involvement of prostaglandin E receptors.** *Carcinogenesis* 2011, **32**:240–245.
9. Mita H, Toyota M, Aoki F, Akashi H, Maruyama R, Sasaki Y, Suzuki H, Idogawa M, Kashima L, Yanagihara K, Fujita M, Hosokawa M, Kusano M, Sabau SV, Tatsumi H, Imai K, Shinomura Y, Tokino T: **A novel method, digital genome scanning detects *KRAS* gene amplification in gastric cancers: involvement of overexpressed wild-type KRAS in downstream signaling and cancer cell growth.** *BMC Cancer* 2009, **9**:198.
10. Feller SM: **Crk family adaptors-signalling complex formation and biological roles.** *Oncogene* 2001, **20**:6348–6371.
11. Birge RB, Kalodimos C, Inagaki F, Tanaka S: **Crk and CrkL adaptor proteins: networks for physiological and pathological signaling.** *Cell Commun Signal* 2009, **7**:13.
12. Yamamoto G, Nannya Y, Kato M, Sanada M, Levine RL, Kawamata N, Hangaishi A, Kurokawa M, Chiba S, Gilliland DG, Koeffler HP, Ogawa S: **Highly sensitive method for genomewide detection of allelic composition in nonpaired, primary tumor specimens by use of affymetrix single-nucleotidepolymorphism genotyping microarrays.** *Am J Hum Genet* 2007, **81**:114–126.
13. Ogawa S, Nanya Y, Yamamoto G: **Genome-wide copy number analysis on GeneChip platform using copy number analyzer for affymetrix GeneChip 2.0 software.** *Methods Mol Biol* 2007, **396**:185–206.
14. Shinmura K, Goto M, Suzuki M, Tao H, Yamada H, Igarashi H, Matsuura S, Maeda M, Konno H, Matsuda T, Sugimura H: **Reduced expression of MUTYH with suppressive activity against mutations caused by 8-hydroxyguanine is a novel predictor of a poor prognosis in human gastric cancer.** *J Pathol* 2011, **225**:414–423.
15. Shinmura K, Iwaizumi M, Igarashi H, Nagura K, Yamada H, Suzuki M, Fukasawa K, Sugimura H: **Induction of centrosome amplification and chromosome instability in *p53*-deficient lung cancer cells exposed to benzo[*a*]pyrene diol epoxide (B[*a*]PDE).** *J Pathol* 2008, **216**:365–374.
16. Sugimura H, Mori H, Nagura K, Kiyose S, Tao H, Isozaki M, Igarashi H, Shinmura K, Hasegawa A, Kitayama Y, Tanioka F: **Fluorescence *in situ* hybridization analysis with a tissue microarray: 'FISH and chips' analysis of pathology archives.** *Pathol Int* 2010, **60**:543–550.
17. Sugimura H: **Detection of chromosome changes in pathology archives: an application of microwave-assisted fluorescence in situ hybridization to human carcinogenesis studies.** *Carcinogenesis* 2008, **29**:681–687.
18. Iwaizumi M, Shinmura K, Mori H, Yamada H, Suzuki M, Kitayama Y, Igarashi H, Nakamura T, Suzuki H, Watanabe Y, Hishida A, Ikuma M, Sugimura H: **Human Sgo1 downregulation leads to chromosomal instability in colorectal cancer.** *Gut* 2009, **58**:249–260.
19. Suzuki M, Nagura K, Igarashi H, Tao H, Midorikawa Y, Kitayama Y, Sugimura H: **Copy number estimation algorithms and fluorescence in situ hybridization to describe copy number alterations in human tumors.** *Pathol Int* 2009, **59**:218–228.
20. Nakamura S, Hirano I, Okinaka K, Takemura T, Yokota D, Ono T, Shigeno K, Shibata K, Fujisawa S, Ohnishi K: **The FOXM1 transcriptional factor promotes the proliferation of leukemia cells through modulation of cell cycle progression in acute myeloid leukemia.** *Carcinogenesis* 2010, **31**:2012–2021.
21. Goto M, Shinmura K, Nakabeppu Y, Tao H, Yamada H, Tsuneyoshi T, Sugimura H: **Adenine DNA glycosylase activity of 14 human MutY homolog (MUTYH) variant proteins found in patients with colorectal polyposis and cancer.** *Hum Mutat* 2010, **31**:E1861–E1874.
22. Rosti G, Castagnetti F, Gugliotta G, Palandri F, Martinelli G, Baccarani M: **Dasatinib and nilotinib in imatinib-resistant Philadelphia-positive chronic myelogenous leukemia: a 'head-to-head comparison'.** *Leuk Lymphoma* 2010, **51**:583–591.
23. Borriello A, Caldarelli I, Bencivenga D, Cucciolla V, Oliva A, Usala E, Danise P, Ronzoni L, Perrotta S, Della Ragione F: **p57Kip2 is a downstream effector of BCR-ABL kinase inhibitors in chronic myelogenous leukemia cells.** *Carcinogenesis* 2011, **32**:10–18.
24. Weisberg E, Manley PW, Breitenstein W, Brüggen J, Cowan-Jacob SW, Ray A, Huntly B, Fabbro D, Fendrich G, Hall-Meyers E, Kung AL, Mestan J, Daley GQ, Callahan L, Catley L, Cavazza C, Azam M, Neuberg D, Wright RD, Gilliland DG, Griffin JD: **Characterization of AMN107, a selective inhibitor of native and mutant Bcr-Abl.** *Cancer Cell* 2005, **7**:129–141.
25. Sugimoto Y, Nakamura S, Okinaka K, Hirano I, Ono T, Shigeno K, Shinjo K, Ohnishi K: **HOXA10 expression induced by Abl kinase inhibitors enhanced apoptosis through PI3K pathway in CML cells.** *Leuk Res* 2008, **32**:962–971.
26. Kardinal C, Konkol B, Schulz A, Posern G, Lin H, Adermann K, Eulitz M, Estrov Z, Talpaz M, Arlinghaus RB, Feller SM: **Cell-penetrating SH3 domain blocker peptides inhibit proliferation of primary blast cells from CML patients.** *FASEB J* 2000, **14**:1529–1538.
27. Sattler M, Salgia R: **Role of the adapter protein CRKL in signal transduction of normal hematopoietic and BCR/ABL-transformed cells.** *Leukemia* 1998, **12**:637–644.
28. ten Hoeve J, Arlinghaus RB, Guo JQ, Heisterkamp N, Groffen J: **Tyrosine phosphorylation of CRKL in Philadelphia + leukemia.** *Blood* 1994, **84**:1731–1736.
29. Nakamura T, Komiya M, Sone K, Hirose E, Gotoh N, Morii H, Ohta Y, Mori N: **Grit, a GTPase-activating protein for the Rho family, regulates neurite extension through association with the TrkA receptor and N-Shc and CrkL/Crk adapter molecules.** *Mol Cell Biol* 2002, **22**:8721–8734.
30. ten Hoeve J, Morris C, Heisterkamp N, Groffen J: **Isolation and chromosomal localization of CRKL, a human crk-like gene.** *Oncogene* 1993, **8**:2469–2474.
31. Kim N, Park WY, Kim JM, Park JH, Kim JS, Jung HC, Song IS: **Gene expression of AGS cells stimulated with released proteins by *Helicobacter pylori*.** *J Gastroenterol Hepatol* 2008, **23**:643–651.
32. Ko JC, Ciou SC, Cheng CM, Wang LH, Hong JH, Jheng MY, Ling ST, Lin YW: **Involvement of Rad51 in cytotoxicity induced by epidermal growth factor receptor inhibitor (gefitinib, Iressa^{R}) and chemotherapeutic agents in human lung cancer cells.** *Carcinogenesis* 2008, **29**:1448–1458.
33. Holden J, Garrett Z, Stevens A: **NICE guidance on trastuzumab for the treatment of HER2-positive metastatic gastric cancer.** *Lancet Oncol* 2011, **12**:16–17.
34. Norell H, Poschke I, Charo J, Wei WZ, Erskine C, Piechocki MP, Knutson KL, Bergh J, Lidbrink E, Kiessling R: **Vaccination with a plasmid DNA encoding HER-2/neu together with low doses of GM-CSF and IL-2 in patients with metastatic breast carcinoma: a pilot clinical trial.** *J Transl Med* 2010, **8**:53.
35. Araujo J, Logothetis C: **Dasatinib: a potent SRC inhibitor in clinical development for the treatment of solid tumors.** *Cancer Treat Rev* 2010, **36**:492–500.

36. Kantarjian HM, Cortes J, La Rosée P, Hochhaus A: **Optimizing therapy for patients with chronic myelogenous leukemia in chronic phase.** *Cancer* 2010, **116**:1419–1430.

doi:10.1186/1479-5876-10-97
Cite this article as: Natsume *et al.*: The *CRKL* gene encoding an adaptor protein is amplified, overexpressed, and a possible therapeutic target in gastric cancer. *Journal of Translational Medicine* 2012 10:97.

Gastric Cancer
DOI 10.1007/s10120-012-0177-y

LETTER TO THE EDITOR

How can research fields be integrated with PET imaging?

Haruhiko Sugimura

Advances in molecular biology have reasonably driven many pathologists and many of those desiring to become pathologists to investigate the molecular characterization of human tumors. Pathologists specializing in gastric cancer are not exceptions. Microsatellite instability (MSI) in the DNA of human cancer cells has attracted the attention of the research community because MSI sometimes reflects constitutive genetic defects in mismatch repair (MMR) genes. Such information is especially important for the diagnosis of colorectal cancer in patients suspected of having hereditary nonpolyposis colorectal cancer (HNPCC) [1]. While MSI itself is characteristic of tumors, it also reflects genetic traits transmitted from one generation to the next.

MSI was previously assumed to play the same role in gastric cancer as it does in colorectal cancer: that is, many researchers expected to observe frequent MSI in familial gastric cancer cases. In most settings, however, this has not been the case. MSI in gastric cancer is known to occur in response to a deficiency in MMR genes because of promoter methylation. The methylation of *MLH1* has been identified in metaplastic gastric mucosa surrounding differentiated adenocarcinoma [2]. Epigenetic changes similar to those occurring in non-tumor gastric mucosa are now being extensively studied in light of their possible use as predictors of the recurrence of gastric cancer after endoscopic submucosal dissection [3]. Of note, the biological and clinical significance of MSI during the advanced stage of gastric cancer has been extensively studied for the past decade. MSI is a molecular marker that is involved in the pathogenesis and progression of gastric cancer either in an independent manner and/or in coordination with pivotal cancer-associated genes, such as *CDH1* and *MET* [4]. Importantly, MSI-positive tumors exhibit changes in the target genes (of the MMR genes) that control critical biological behaviors in tumors [5]. Despite these expectations regarding the use of MSI as a clinically feasible marker, neither clinicians nor pathologists have regarded MSI as a critical factor on which clinical decisions must be based. How do other members of the clinical team view the contribution of MSI? Diagnostic radiologists are usually not familiar with MSI (based on my personal experience), and imaging radiology has been one of the disciplines farthest from research fields examining genetic aberrations in tumors.

In this issue of *Gastric Cancer*, the work of an interdisciplinary team at the Konkuk University School of Medicine in Seoul, Korea, is reported (Chung et al. [6]); this team has integrated the above-mentioned research fields, combining positron emission tomography (PET) findings with MSI status for the diagnosis of gastric cancer6. Because researchers at this university have continuously reported data on MSI in colorectal and gastric cancer, their data for MSI in gastric cancer is accumulating [7]. Whether Chung et al. [6] intentionally compared PET data and MSI findings or whether their encounter with this correlation was serendipitous is not clear. The key findings of their study were that the presence of fluorodeoxyglucose (FDG) uptake on PET/computed tomography (CT) images ($P = 0.001$) and a higher maximum standardized uptake value (SUVmax) in gastric cancer was linked to the presence of MSI ($P < 0.001$). Many PET researchers have been trying to correlate PET findings with tumor phenotypes [8], but matching such findings to the molecular nature of

This editorial refers to the article doi:10.1007/s10120-012-0165-2.

H. Sugimura (✉)
Department of Tumor Pathology, Hamamatsu University School of Medicine, Hamamatsu, Japan
e-mail: hsugimur@hama-med.ac.jp

Published online: 18 July 2012

tumors is not an easy achievement in clinical settings, even though many clinicians are aware that MSI can provide useful information regarding tumors that is highly relevant to the present-day management of patients.

One straightforward interpretation of the findings of Chung et al. would be that the apparent association they found between PET/CT detectability and MSI is a secondary effect arising from the tumor size and other factors. Actually, PET/CT detectability is related to the patient's age and the size of the tumor. MSI is also known to be prevalent in advanced gastric cancers among the elderly [9]. Even though the apparent association between PET/CT detectability and MSI could be a secondary coincidence, the reported findings provide several insights as to why this association occurs. FDG-PET/CT detects areas with high glucose intake, which is dependent on the activity of the glucose transporter 1 (GLUT1) protein. The report by Chung et al. [6] in this issue of the journal does not provide GLUT1 (SLC 2A1) expression data, although they mentioned on that; however, several reports have shown GLUT1 overexpression in human tumors. *GLUT1* is located at 1p34, in the vicinity of many genes associated with gastric cancer (including *EPHA8*, *EPHB2*, *TIE*, and *MYH*), and GLUT1 expression in gastric cancer may be related to the phenomenon reported by Chung et al. [6]. This perspective may have broader implications regarding the molecular natures of tumors in terms of personalized therapeutics. GLUT1 is one of the most frequently increased transcripts in colorectal cancer with the *BRAF* mutation [10], which is a molecular marker highly relevant to personalized therapy for colorectal cancer. Thus, PET positivity and its correlation with MSI may be the first theranostic [11] finding in the field of gastric cancer research and practice. Not many modalities for personalized therapy for gastric cancer, other than human epidermal growth factor receptor 2 (HER2)-Herceptin (trastuzumab), are available at present, but a wider variety of markers, including MSI and associated features, are likely to be available in the near future. For optimists, the information reported here indicating that PET may disclose potentially manipulable characteristics of the gastric cancer genome is encouraging.

References:

1. Goodenberger M, Lindor NM. Lynch syndrome and MYH-associated polyposis: review and testing strategy. J Clin Gastroenterol. 2011;45:488–500.
2. Guo RJ, Arai H, Kitayama Y, et al. Microsatellite instability of papillary subtype of human gastric adenocarcinoma and hMLH1 promoter hypermethylation in the surrounding mucosa. Pathol Int. 2001;51:240–7.
3. Maekita T, Nakazawa K, Mihara M, et al. High levels of aberrant DNA methylation in *Helicobacter pylori*-infected gastric mucosae and its possible association with gastric cancer risk. Clin Cancer Res. 2006;12:989–95.
4. Yokozaki H, Yasui W, Tahara E. Genetic and epigenetic changes in stomach cancer. Int Rev Cytol. 2001;204:49–95.
5. Shah SN, Hile SE, Eckert KA. Defective mismatch repair, microsatellite mutation bias, and variability in clinical cancer phenotypes. Cancer Res. 2010;70:431–5.
6. Chung HW, Lee S-Y, Han HS, et al. Gastric cancers with microsatellite instability exhibit high fluorodeoxyglucose uptake in positron emission tomography. Gastric Cancer. 2012.
7. Lee SY, Chung H, Devaraj B, et al. Microsatellite alterations at selected tetranucleotide repeats are associated with morphologies of colorectal neoplasias. Gastroenterology. 2010;139:1519–25.
8. Tsujikawa T, Yoshida Y, Maeda H, et al. Oestrogen-related tumour phenotype: PET characterisation with 18F-FDG and 18F-FES. Br J Radiol. 2010.
9. Wang Y, Shinmura K, Guo RJ, et al. Mutational analyses of multiple target genes in histologically heterogeneous gastric cancer with microsatellite instability. Jpn J Cancer Res. 1998;89:1284–91.
10. Yun J, Rago C, Cheong I, et al. Glucose deprivation contributes to the development of KRAS pathway mutations in tumor cells. Science. 2009;325:1555–9.
11. Niu G, Chen X. Molecular imaging with activatable reporter systems. Theranostics. 2012;2:413–23.

INTERNAL MEDICINE

□ CASE REPORT □

An Autopsy Case of Malignant Pleural Mesothelioma Associated with Nephrotic Syndrome

Seiichiro Suzuki[1], Mikio Toyoshima[1], Fumiya Nihashi[1], Hiroe Tsukui[2], Satoshi Baba[2], Haruhiko Sugimura[3] and Takafumi Suda[4]

Abstract

A 64-year-old man who had been exposed to asbestos was referred to our hospital for a detailed examination of left pleural effusion. A laboratory examination of the urine and blood revealed nephrotic syndrome. A thoracoscopic examination did not yield a definitive diagnosis. Twenty months later, a left pleural tumor became apparent, and the patient died of respiratory failure and cachexia. An autopsy revealed epithelioid malignant pleural mesothelioma. The glomeruli appeared normal under light microscopy. A review of the English literature revealed only three reports of malignant mesothelioma associated with minimal-change nephrotic syndrome. The natural course of malignant mesothelioma with nephrotic syndrome has not been previously reported.

Key words: malignant mesothelioma, minimal-change nephrotic syndrome, paraneoplastic syndrome

(Intern Med 53: 243-246, 2014)
(DOI: 10.2169/internalmedicine.53.1313)

Introduction

Malignant mesothelioma is an asbestos-associated neoplasm of serous membranes, such as the pleura and peritoneum. In contrast to primary lung cancer (1), information regarding paraneoplastic syndromes associated with malignant mesothelioma is limited (2). We herein describe an autopsy case of malignant pleural mesothelioma associated with nephrotic syndrome and discuss possible correlations between malignant mesothelioma and nephrotic syndrome with a review of the English literature.

Case Report

A 64-year-old man was referred to our hospital for a detailed examination of left pleural effusion detected on chest radiography as part of a mass screening examination. He was asymptomatic; however, he had a 40-pack-year history of smoking. He had also worked at an asbestos products manufacturer for 10 years during his thirties and had been exposed to asbestos fibers. His personal history included multiple brain infarctions and mild dementia. A physical examination revealed pitting edema in both legs, which had appeared two months prior to presentation at our hospital. His body weight had increased from 59.4 kg to 62.0 kg during those two months. The laboratory data showed normal urine sediment with no evidence of casts in addition to positive urine protein (9.7 g/day), hypoproteinemia (serum total protein, 5.0 g/dL), hypoalbuminemia (serum albumin, 1.9 g/dL) and hyperlipidemia (total cholesterol, 275 mg/dL), suggesting nephrotic syndrome. His renal function was normal (blood urea nitrogen, 18 mg/dL; and serum creatinine, 1.0 mg/dL). Additional laboratory studies revealed normal levels of C3 and C4 with no evidence of rheumatoid factor. No antibodies against double-stranded DNA, antinuclear antibodies, antineutrophil cytoplasmic autoantibodies or antiglomerular basement membrane antibodies were detected. Serum protein electrophoresis and immunoglobulin (Ig) bands on immunoelectrophoresis were normal. The serum levels of IgA and IgM were within the normal limits, while the IgG levels were depressed (795 mg/dL). Negative results

[1]Department of Respiratory Medicine, Hamamatsu Rosai Hospital, Japan, [2]Department of Diagnostic Pathology, Hamamatsu University School of Medicine, Japan, [3]Department of Tumor Pathology, Hamamatsu University School of Medicine, Japan and [4]The Second Department of Internal Medicine, Hamamatsu University School of Medicine, Japan
Received for publication July 6, 2013; Accepted for publication September 2, 2013
Correspondence to Dr. Mikio Toyoshima, mi-toyoshima@hamamatsuh.rofuku.go.jp